Response to Anonymous Referee #1

Referee #1

This is a well-written manuscript of an important topic that deserves publication after some minor modifications.

Response:

We greatly appreciate the referee for taking precious time in providing the detailed comments. We tried our best to carefully account for all comments from the referee that will certainly improve the manuscript and supplement. We hope that the revised manuscript and supplement meet the standards of the referee. Basically, responses are provided with detailed explanations for each comment. Where multiple comments could be addressed together, we provided a collective response. Meanwhile, for simple minor suggestions such as word additions, deletions, or substitution, we listed only the revised sentences. Once again, we deeply thank the referee's valuable comments; all modifications in the main text are highlighted in blue.

[Comments 1]

Can you make any statements about cloudiness within the various areas? This would relate to the accumulation mode. Perhaps it was more cloudy in the Indian Ocean since there was more precipitation.

Response:

Thanks for the suggestion on cloudiness. Unfortunately, direct measurements of cloud fraction were not conducted during the transit voyage of the R/V *ISABU* in 2024. Alternatively, we attempted to indirectly estimate cloudiness using Pyrgeometer observations. Nevertheless, a simple comparison of the raw values is unfeasible due to the regional variability of factors influencing longwave radiation, including temperature, RH, and SST. Therefore, based on Equation S10, we estimated the clear-sky downward longwave radiation (Ldn_{clear}) and calculated the anomalies (ΔLdn) from the Pyrgeometer ($PYRGE$) data for comparison.

Consequently, as suspected by the referee, the cloudiness (i.e., ΔLdn) was higher in the Indian Ocean than in other regions (Fig. S6). These findings confirm that high aerosol or CCN number concentrations do not necessarily lead to cloud formation in real environments. Moreover, we examined the spatial distributions of cloudiness (Fig. R1). However, as the number concentrations of accumulation mode also varied significantly across various sea areas, a direct correlation between cloudiness and the accumulation mode could be identified only in

specific sectors of the Indian Ocean.

In conclusion, we summarized and added only the former results to the manuscript and supplement.

"In addition, the cloudiness estimated from downward longwave radiation was also higher in the Indian Ocean than in other regions (Fig. S6). This provides indirect evidence that high N_{CN} (especially accumulation mode) or N_{CCN} do not always result in cloud formation in moisture-limited real environments because of the competition for available water vapor." (lines 295–9 in the manuscript)

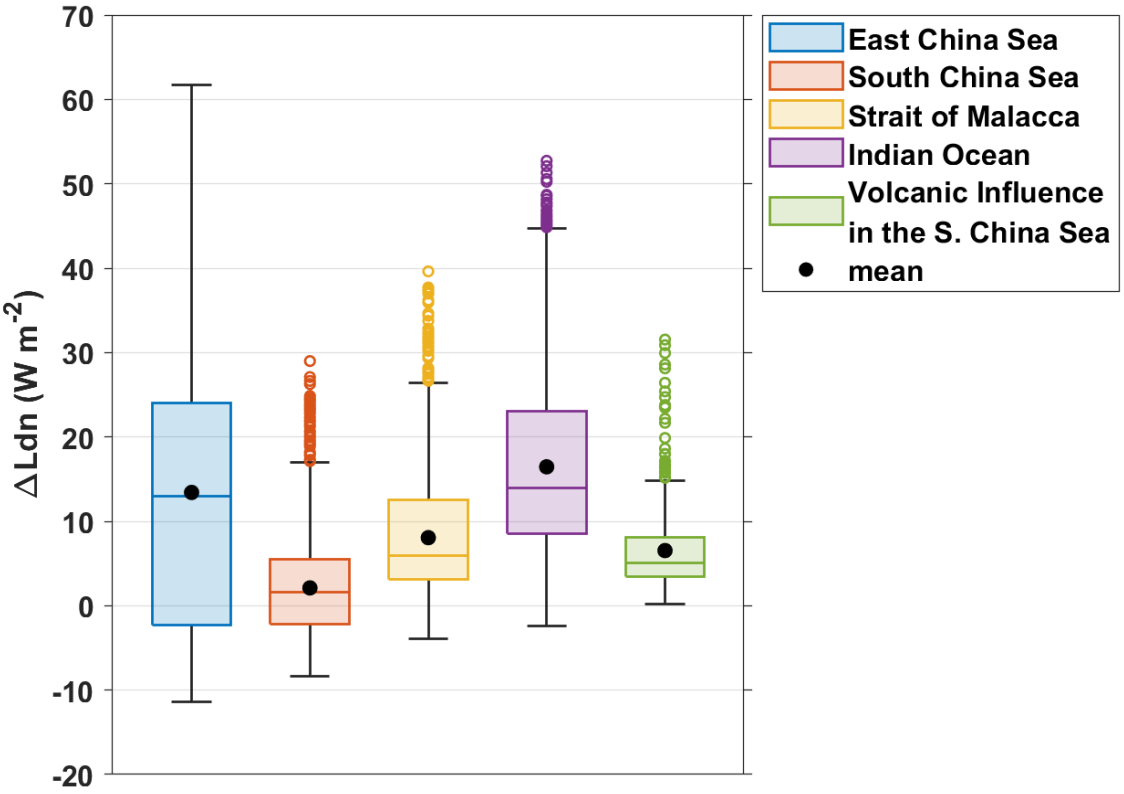

Figure S6. Box plots of ΔLdn for each sea area. For the South China Sea, the volcanic-influence period was depicted separately. Black dots represent the mean values. The horizontal line in each box and the black dots represent the median and mean values, respectively. The range of the boxes is from 25th percentile to 75th percentile (IQR). The whiskers extend away from the box to the two extreme values but if there are data points that exceed $1.5 \times IQR$ from the upper or lower end of the box, they are shown as colored dots as outliers.

"ΔLdn represents the difference between the total downward longwave radiation ($PYRGE$) measured by a Pyrgeometer and the calculated clear-sky downward longwave radiation (Ldn_{clear}). In the absence of direct cloud observations, cloudiness was indirectly estimated using longwave radiation. However, since longwave radiation is significantly influenced by temperature, RH, and sea surface temperature, we calculated Ldn_{clear} based on Equation S10 to extract the effect of clouds and ultimately used anomalies for the analysis.

$$e_s(kPa) = 0.6108 \cdot \exp\left(\frac{17.27 \cdot T(℃)}{T(℃)+237.3}\right),$$

$$e_a(hPa) = \frac{RH}{100} \cdot e_s(kPa) \cdot 10,$$

$$\varepsilon_{a,clear} = 1.24 \left(\frac{e_a(hPa)}{T(K)}\right)^{\frac{1}{7}} \text{ (Brutsaert equation)},$$

$$Ldn_{clear} = \varepsilon_{a,clear} \sigma T(k)^4,$$

$$\Delta Ldn = PYRGE - Ldn_{clear}, \quad \text{(S10)}$$

where T and RH are temperature and relative humidity, respectively. e_s and e_a indicate the saturation vapor pressure and actual vapor pressure, respectively. $\varepsilon_{a,clear}$ represents the effective clear-sky emissivity, which was calculated in this study using the Brutsaert equation. $\sigma = 5.67 \times 10^{-8}\, W\, m^{-2} K^{-4}$ is the Stefan – Boltzmann constant." (lines 204–18 in the supplement)

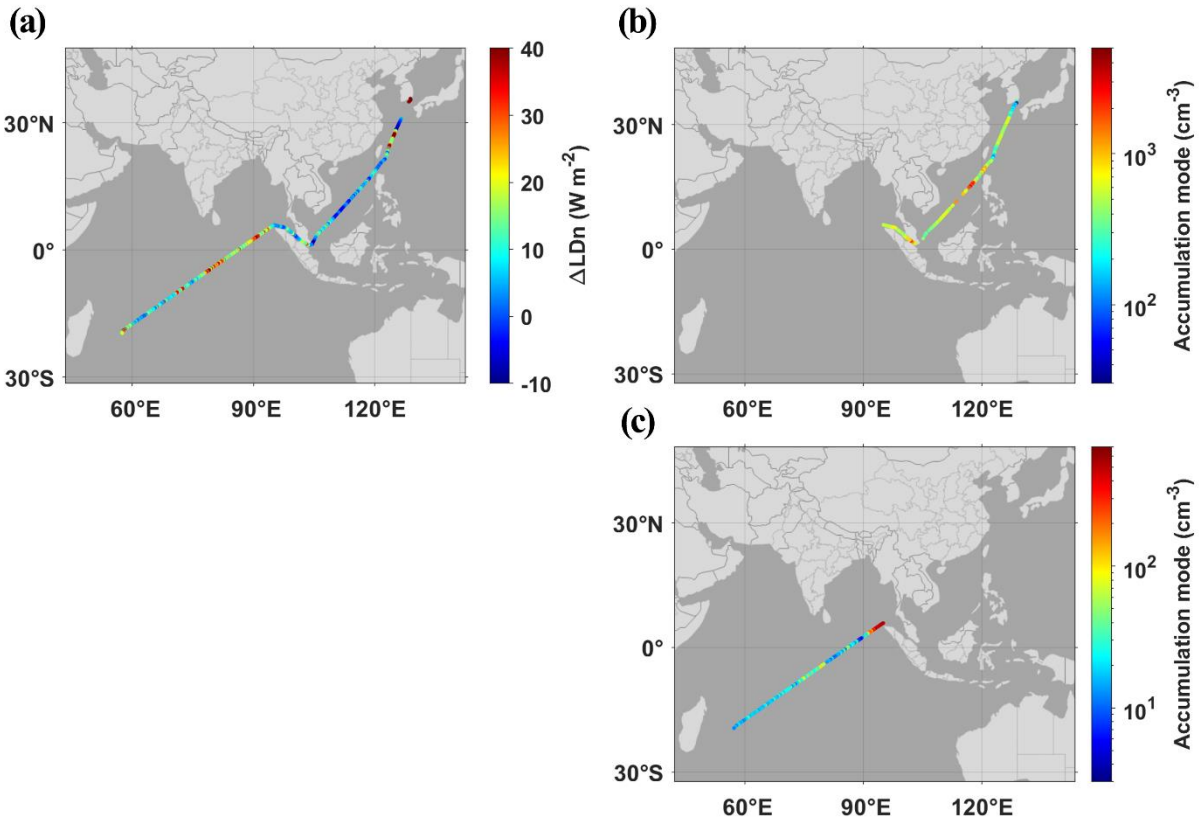

Figure R1. Spatial distributions of (a) ΔLdn and number concentrations of accumulation mode over (b) the East China Sea, South China Sea, and Strait of Malacca, and (c) the Indian Ocean. Note that the Indian Ocean and the other regions are plotted separately due to the significant difference in their number concentrations. This figure is used exclusively in this response, so we designated this figure as Figure R1.

[Minor Comments on Figures and Tables in Manuscript]

Fig. 2. *Is there a significance to the white strip at 15°N latitude?*

Response:

We have double–checked Figure 1 (originally Figure 2) and found no specific white strip at 15°N latitude. Aside from the referee's comment, regional information is added to Figure 1.

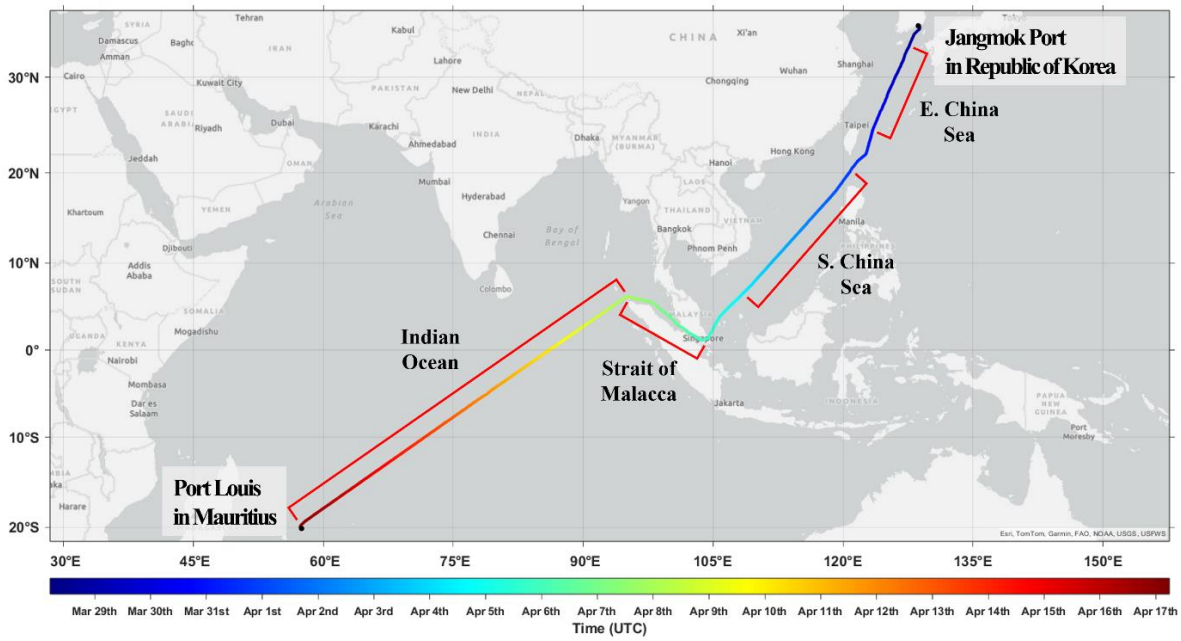

Figure 1. Cruise route of the R/V *ISABU* in 2024, including regional classification (Source: Esri, TomTom, Garmin, FAO, NOAA, USGS, USFWS; Powered by Esri).

Fig. 4a. *Explain gaps.*

Response:

Thank for pointing this out. As described in Step 2 of Section S1, some anomalous observation data points did not show an abrupt increase in the QOF which is the correction criterion. So, we excluded these data from this study and represented them as gaps in Fig. 3a and b (originally Fig. 4a and b). Accordingly, we added this explanation to the caption as follows:

"In (a) and (b), aerosol data gaps imply that there are anomalous observation data excluded from this study as they did not satisfy the correction criteria." (lines 340–2)

Fig. 4b. *Reverse the legend order for N_{CCN}. 1% should be closest to N_{CN}.*

Response:

Done as suggested.

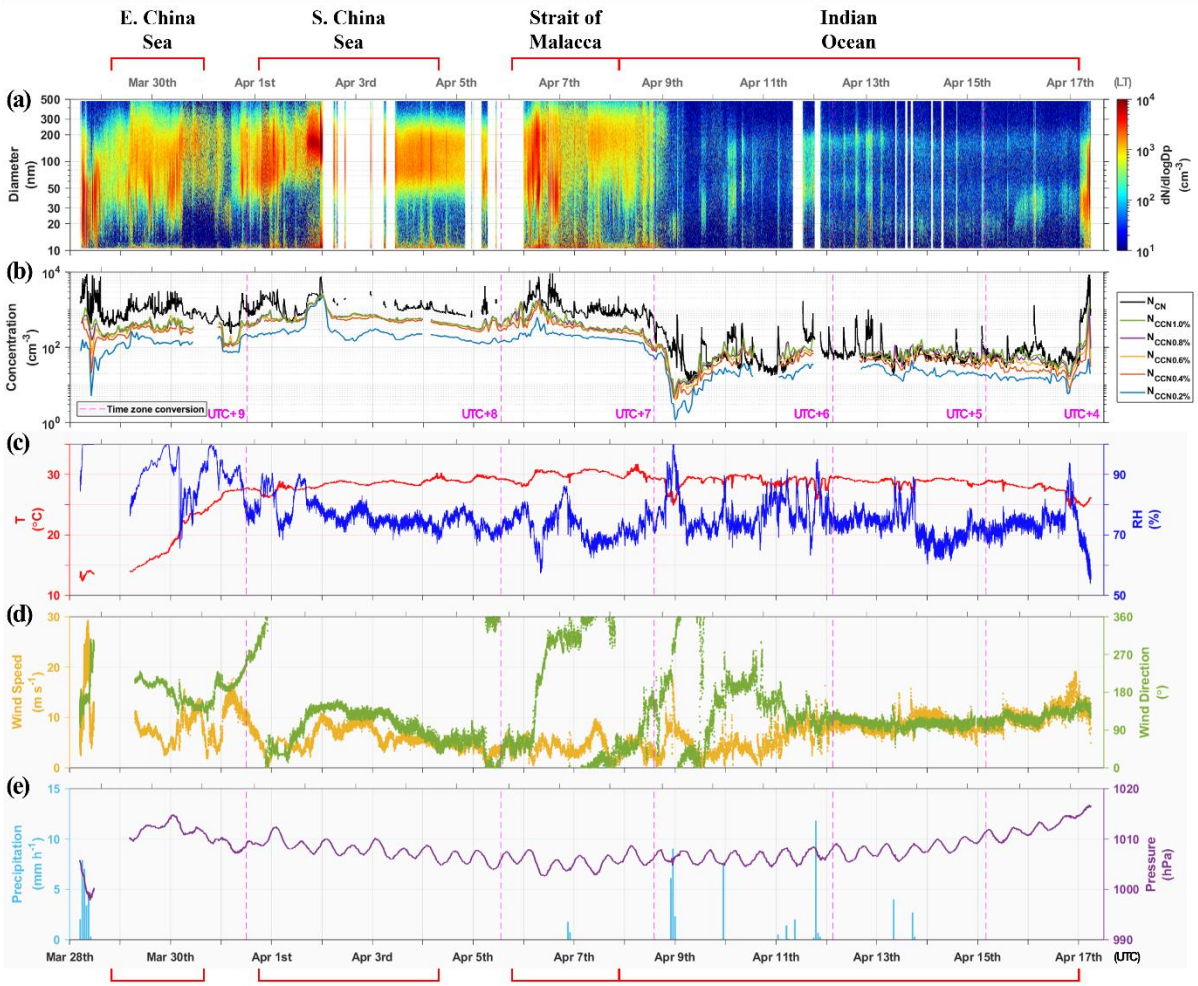

Figure 3. Time series of (a) aerosol size distribution, (b) total aerosol and CCN number concentrations, (c) temperature and relative humidity (RH), (d) true wind speed and direction, and (e) precipitation and pressure during the transit voyage of the R/V *ISABU*. The top and bottom x-axis are Local Time (LT) and Coordinated Universal Time (UTC), respectively, and the x-axis tick marks indicate the midnight of each day. In (a) and (b), aerosol data gaps imply that there are anomalous observation data excluded from this study as they did not satisfy the correction criteria. The vertical magenta dashed lines indicate the changes in the local time zone, with the applied time zone for each segment presented in (b).

Fig. 5. *Explain NCN15. Apparently means all particles larger than 15 μm.*

Response:

N_{CN15} in the figures represents the total number concentration of aerosols larger than 15 nm. To ensure consistency with the main text, where N_{CN} is used throughout, we revised N_{CN15} to N_{CN} in Figures 3, 4, 5, 7, and 8 (originally Figures 4, 5, 6, 8, and 9). Then, we added a detailed definition of N_{CN} in Section 2.1.2. We also revised figure captions accordingly.

"Accordingly, N_{CN} in this study refers to the total number concentration of aerosols larger than 15 nm." (lines 152–3)

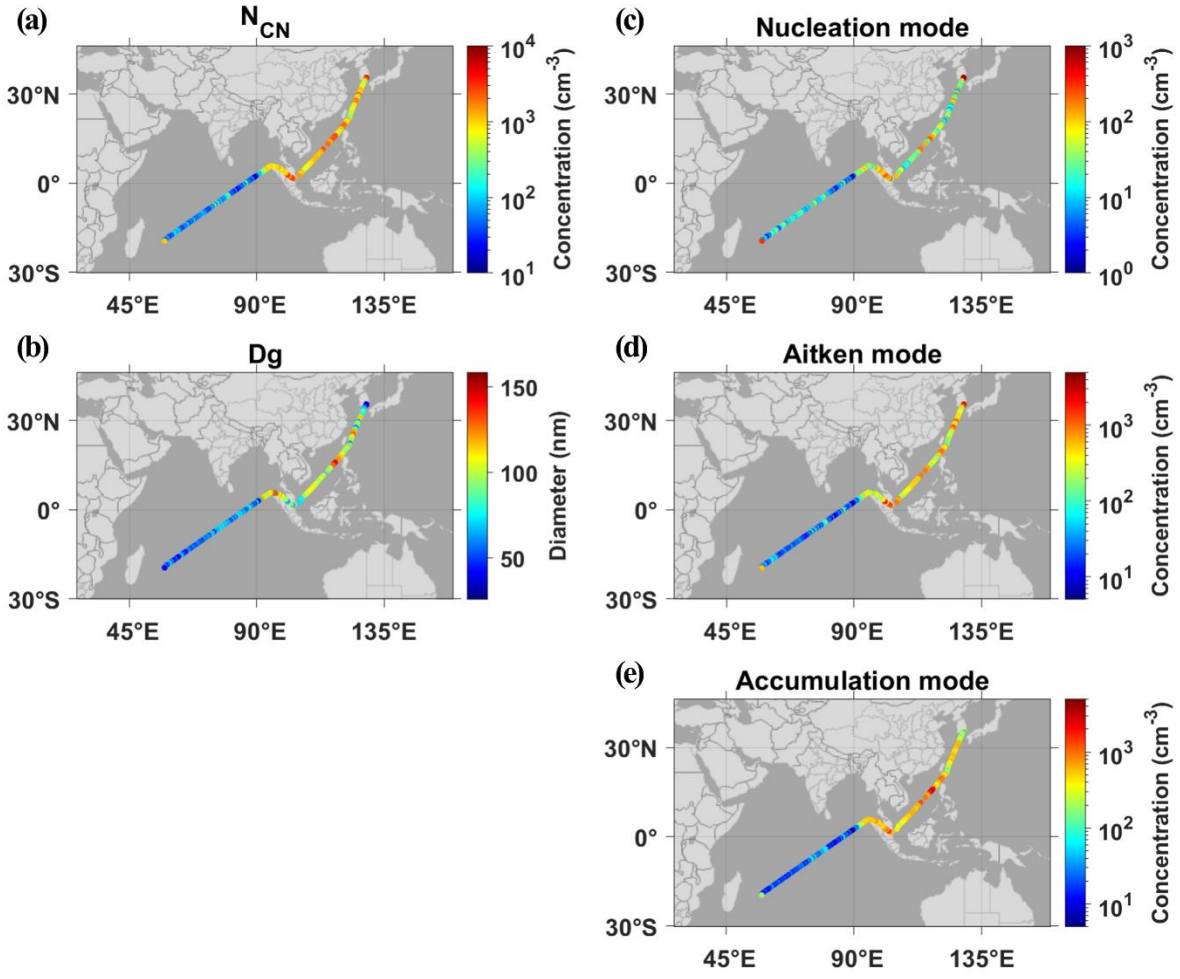

Figure 4. Spatial distributions of (a) total aerosol number concentrations, (b) geometric mean diameter, and number concentrations of (c) nucleation mode (15–25 nm), (d) Aitken mode (25–100 nm), and (e) accumulation mode (100–500 nm) during the transit voyage of the R/V *ISABU* (from Natural Earth).

Fig. 8. *These types of plots require explanation. What is the horizontal line within each box? Probably a median but for just the box or all data. What range do the boxes include, perhaps standard deviation. What range do the extreme lines represent, perhaps 90% of data. What do the out of box data represent? Label nucleation, Aitken and accumulation.*

Response:

We followed the convention of the "schematic plot" introduced in Wilks (2011). Briefly this is explained in captions of Figures 7 and 8 (originally Figures 8 and 9) as the referee suggested. We also revised labels in Figure 7c–e (originally Figure 8c–e) as the referee suggested. Furthermore, we have revised the captions for the box plots in the supplement.

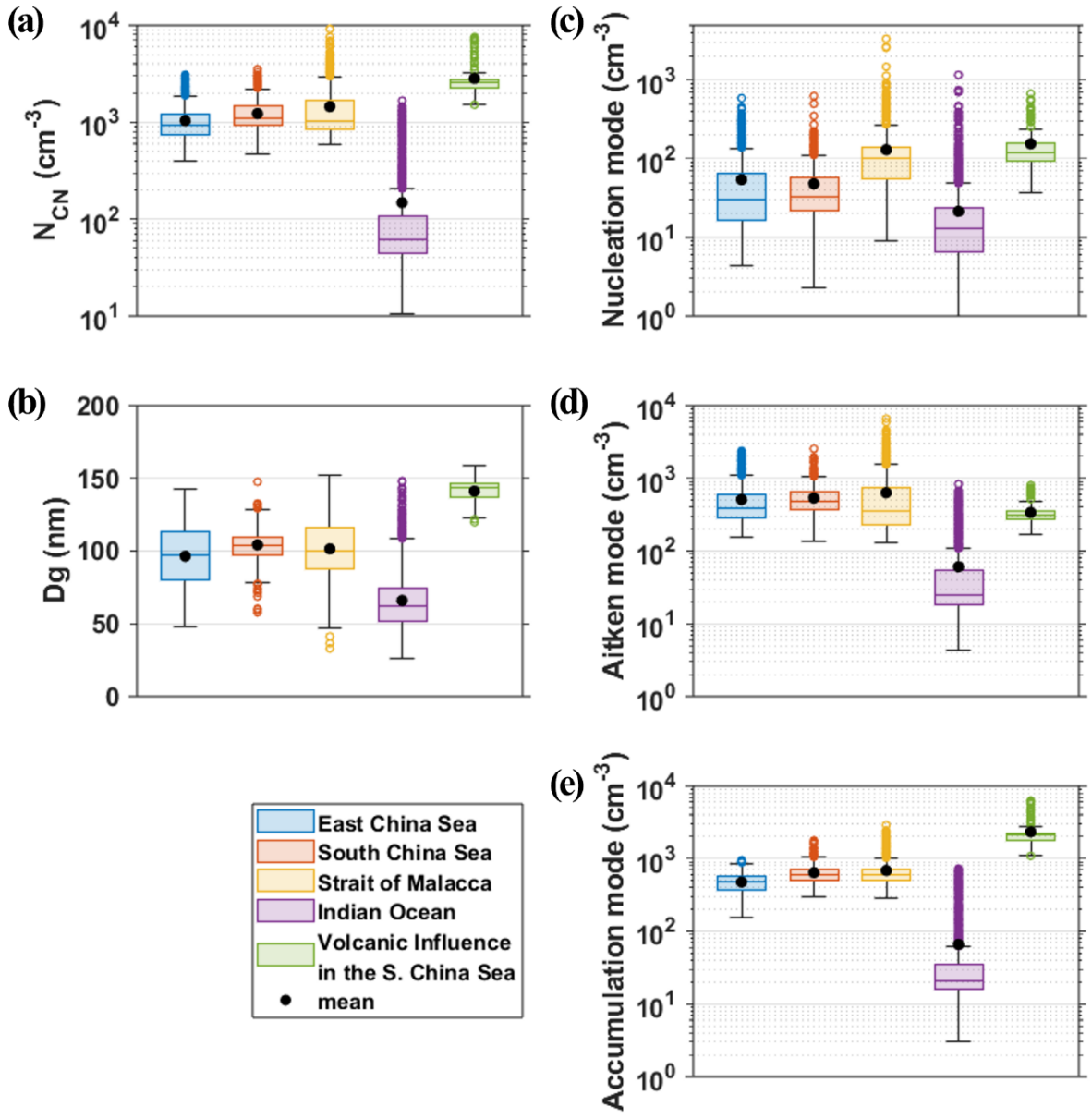

Figure 7. Box plots of (a) total aerosol number concentrations, (b) geometric mean diameter, and (c) nucleation (15–25 nm), (d) Aitken (25–100 nm), and (e) accumulation (100–500 nm) mode number concentrations for each sea area. For the South China Sea, the volcanic-influence period was depicted separately. The horizontal line in each box and the black dots represent the median and mean values, respectively. The range of the boxes is from 25th percentile to 75th percentile (IQR). The whiskers extend away from the box to the two extreme values but if there are data points that exceed $1.5 \times IQR$ from the upper or lower end of the box, they are shown as colored dots as outliers.

Fig. 11. *Is difficult to read. Log scale for vertical would help. The star symbol in the legend is much smaller than within the figure. Please enlarge to same size so it is readable.*

Response:

Following the referee's comments, we converted the y-axis to a log scale and revised the symbols in the legend for better visibility.

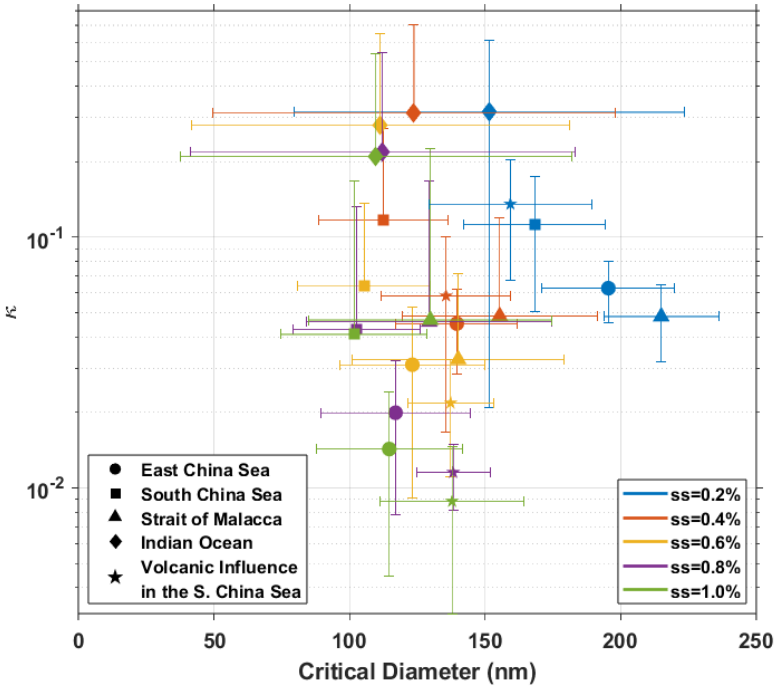

Figure 10. Distributions of the D_C and κ at given supersaturations for each sea area. The symbols represent the mean values, and the lengths of the error bars correspond to one standard deviation. For the South China Sea, the volcanic-influence period was depicted separately.

Table. 1. *Add a column for mean N_{CN}.*

Response:

A N_{CN} column has been inserted next to the 'Sea Area' column, and the title has also updated accordingly.

Table 2. Total aerosol number concentrations and the coefficients of determination and parameters of CCN fitting for each sea area.

	N_{CN}	$N_{CCN} = C \times SS^{\alpha}$			$N_{CCN} = N \times (1 - exp(-B \times SS^{\beta}))$			
	(cm^{-3})	R^2	C	α	R^2	N	B	β
East China Sea	1039	0.914	413.1	0.517	0.999	388.4	4.726	1.443
South China Sea	1226	0.783	681.6	0.449	0.998	616.6	13.77	2.089
Strait of Malacca	1449	0.948	678.1	0.561	0.997	664.4	3.367	1.287
Indian Ocean	148	0.967	84.73	0.555	1.000	86.9	2.71	1.148
Volcanic influence in the S. China Sea	2834	0.710	1787	0.097	0.995	1734	45.86	1.997

Note. For the South China Sea, the volcanic-influence period was depicted separately.

Table. 2. *Insert Mean in front of aerosol.*

Response:

Done as suggested.

"Table 3. Mean aerosol number concentrations and geometric mean diameter, CCN number concentrations, and the CCN-to-aerosol ratio for each cluster in each sea area." (line 675)

[Minor Comments on Sentences in Manuscript]

L37–8. *Include concentration.*

Response:

We extensively revised the first three paragraphs of the Introduction to better align them with the scope of this study. In the process, we also incorporated the referee's comments as follows.

"Atmospheric aerosols play a critical role in cloud formation and evolution by acting cloud condensation nuclei (CCN), thereby influencing cloud droplet concentration and size, albedo, cloud lifetime, and precipitation efficiency (Twomey, 1974; Albrecht, 1989)." (lines 34–6)

L196. *Insert ship before plume stack. Delete relatively.*

Response: "First, since the ship plume stack was located behind the observation room, measurements might be contaminated by the vessel's exhaust when the wind blew rapidly from the stern (Fig. 2a)." (lines 180–2)

L234. *Insert The before hygroscopicity.*

Response: "The hygroscopicity parameter (κ) represents the relationship between dry diameter and CCN activity and was calculated according to Petters and Kreidenweis (2007):" (lines 244–5)

L291. *Remove r from larger.*

Response:

In response to all the referees' comments, we revised the sentence as follows.

"A crucial point is that this period was the only instance in which the N_{CCN} at 0.2% SS, where only relatively large aerosols can activate, were similar to N_{CCN} at the other supersaturations (Fig. 3b)." (lines 303–6)

L293. *Remove in.*

Response: "In fact, this enhancement was primarily driven by the accumulation mode (Fig. 4e), particularly by particles around 200 nm diameter, consistent with the distribution of geometric mean diameter (Dg) presented in Fig. 4b." (lines 306–8)

L302. *Change distribution to concentration.*

Response: "N_{CCN} at 0.2% SS exhibited a relatively uniform concentration within the strait, whereas N_{CCN} at the other supersaturations were higher upon entering the strait (at 0.6% SS, 753 ± 404 cm^{-3} when entering vs. 332 ± 57 cm^{-3} when exiting), consistent with the pattern of N_{CN}." (lines 318–21)

L323. *Insert total before aerosol.*

Response: "**Figure 4.** Spatial distributions of (a) total aerosol number concentrations, (b) geometric mean diameter, and number concentrations of (c) nucleation mode (15–25 nm), (d) Aitken mode (25–100 nm), and (e) accumulation mode (100–500 nm) during the transit voyage of the R/V *ISABU* (from Natural Earth)." (lines 346–9)

L415. *Insert than the Strait of Malacca after Sea.*

Response: "The N_{CCN}/N_{CN} ratios at both supersaturations were likewise higher in the South China Sea than the Strait of Malacca." (lines 441–3)

L417–8. *Need explanation.*

Response:

The size, specifically the geometric mean diameter, is a key factor in determining the activation of aerosols into CCN. It is remarkably similar between the South China Sea and the Strait of Malacca. Therefore, it can be inferred that the N_{CCN}/N_{CN} ratios in these two regions were primarily governed by κ. Since the N_{CCN}/N_{CN} ratios in the South China Sea are higher than those in the Strait of Malacca, the aerosols over the South China Sea are considered to be more hygroscopic. A likely reason for the lower κ in the Strait of Malacca is the significant emission of hydrophobic ship exhaust. Since the explanation for this sentence was insufficient as the referee commented, we added further description as follows:

"Nevertheless, considering the similarity in the geometric mean diameter between the two regions (Fig. 7b), the difference in the N_{CCN}/N_{CN} ratios could be primarily governed by κ. This suggests that aerosols in the South China Sea were more hygroscopic and therefore more readily activated as CCN than those in the Strait of Malacca. The major source of aerosols in the Strait of Malacca is the substantial ship emissions emitted from heavy cargo traffic (Saputra et al., 2013; Geng et al., 2023). Given that such emissions are typically hydrophobic, it is reasonable to expect the lower κ values in the Strait of Malacca than in the South China Sea." (lines 445–51)

L422. *Change These to Those.*

Response: "Those ranges were comparable to the results of this study (Fig. 8a–b and Fig. S9a)." (lines 445–6)

L457. *Insert only before in.*

Response:

This sentence was removed during the revision of the manuscript.

L483. *Change increase to are greater.*

Response: "Note that at lower supersaturations, the uncertainties in CCN measurements are greater." (lines 533–4)

L489. *Remove the. Change for each sea area decreased with increasing to is smaller for higher. This is true regardless of sea area.*

Response: "According to Köhler theory, higher supersaturations allow progressively smaller particles to activate; consequently, D_C is smaller for higher supersaturation." (lines 539–40)

L507. *Remove that.*

Response: "Although the κ calculation methods differ, the κ in the South China Sea reported in previous studies (Atwood et al., 2017; Ou et al., 2025) was higher than those obtained in this study." (lines 556–8)

L517–8. *Move Fig. 12 to beginning of sentence.* & **L517**. *Change The to shows. Delete are shown. Change together to along. Remove those. Change fitted to fittings. Remove a.* & **L518**. *Remove as shown in. Add e to 1st formula (plural). Period after formulae.*

Response: "Figure 11 shows measured mean CCN spectra along with fittings by two- and three-parameter formulae." (lines 568–9)

L518. *Insert The before Twomey.* & **L519**. *Change was used as to is.*

Response: "The Twomey formula $N_{CCN} = C \times SS^{\alpha}$ (Twomey, 1959), where C and α are the fitting parameters, is the two-parameter formula." (lines 569–70)

L519–21. *Move a three parameter formula to the beginning of sentence.* & **L520**. *Insert was before proposed.* & ***L521***. *Remove was used as.*

Response: "A three-parameter formula $N_{CCN} = N \times (1 - exp(-B \times SS^{\beta}))$ was proposed by Ji and Shaw (1998), where N, B, and β are the fitting parameters." (lines 570–2)

L521. *Change the to These.* & **L522**. *Change the to these. Fitting plural.*

Response: "These parameters and coefficients of determination for these fittings are summarized in Table 2." (lines 572–3)

L538. *Period after supersaturation. Change and to* β.

Response: "Parameter β reflects the sensitivity of N_{CCN} to supersaturation. β is directly related to D_C." (line 589)

L539. *Remove A. Add s to respond. Delete small changes in. Insert variations after supersaturation.*

Response: "Larger β indicates that N_{CCN} responds more strongly to supersaturation variations." (line 590)

L540. *Particularly to especially.*

Response: "The effect associated with differences in β was especially evident when comparing the South China Sea and the Strait of Malacca." (lines 590–2)

L545. *Change compared to to than in.*

Response: "This contrast could be attributed to the smaller and narrowly distributed D_C and the higher κ in the South China Sea than in the Strait of Malacca, leading to stronger supersaturation-dependent aerosol activation." (lines 594–6)

L547. *Change fluctuations of differences.*

Response: "These differences in β suggest that variations in updraft velocity or subtle changes in thermodynamic conditions can induce substantial differences in cloud microphysics." (lines 597–8)

L549. *Delete In the case of. Capitalize the before Indian. Change when compared with to mean CCN spectra of this study are similar to some of the. Remove conducted.* & **L549–50**. *Move CCN in front of measurements.* & **L550**. *Remove below the BL (this would be submarine). Move 1999 in front of INDOEX. Delete in.* & **L550–1**. *Move parenthetical phrase right after campaign. Remove spectra in this study were similar to those. Period after parenthetical.*

Response: "In the Indian Ocean, mean CCN spectra of this study are similar to some of the aircraft CCN measurements during the 1999 INDOEX campaign (Hudson and Yum, 2002)." (lines 599–600)

L551. *(new sentence). These were classified as 'Clean' at low altitudes south of the ITCZ over the Indian Ocean.*

Response: The corresponding sentence has been added to (lines 600–1).

L552. *Change the to these.* & **L553**. *Change last ocean to area.*

Response: "Considering the gap of more than 20 years between these two observation periods, this consistent result provides strong evidence that the Indian Ocean is a pristine remote area." (lines 602–3)

L562. *Move during the cruise to beginning of sentence. Move air mass origins in front of even. Delete the. Delete of. Period after differ.*

Response: "During the cruise, air mass origins, even within the same sea area, could differ." (line 614)

L562–3. *Change which in turn may lead to to Such. Change in to could affect.*

Response: "Such variations could affect the observed characteristics of aerosols and CCN." (lines 614–5)

L565. *Change were to are.*

Response: "The cluster numbers are assigned in chronological order." (lines 616–7)

L566. *Change classified to divided.*

Response: "The East China Sea was divided into three clusters: seas near Korea (Cluster 1), Mainland China (Cluster 2), and the Pacific Ocean (Cluster 3)." (lines 618–9)

L567–8. *Insert the after to. Move relatively low altitudes right after the. Insert of before Cluster. Remove which remained at.* & **L568**. *Change exceeding to above.*

Response: "In contrast to the relatively low altitudes of Cluster 3, Clusters 1 and 2 were transported from altitudes above 1000 m." (lines 619–20)

L575–6. *Probably sea salt, NaCl.*

Response: "Furthermore, it can be inferred that marine-origin aerosols are likely composed of more hygroscopic components, including sea salt such as NaCl, than continental aerosols." (lines 627–8)

L577. *Insert also after were.* & **L579**. *Change those to air.*

Response: "For the South China Sea, three clusters were also identified: stagnant air masses near the Philippines and Taiwan (Cluster 1); air masses originating from the western Pacific that passed over Luzon Island (Cluster 2); and air that passed over the Visayas Islands (Cluster 3)." (lines 629–31)

L580. *Remove the. Remove of. Move characteristics after CCN. Aerosol singular.*

Response: "Although all three clusters were of marine origin, aerosol and CCN characteristics varied significantly depending on the regions traversed by the air masses." (lines 632–3)

L592. *Cluster plural. Change the to all. Delete somewhat.*

Response: "At other supersaturations, N_{CCN} were comparable between Clusters 1 and 3, although all N_{CCN}/N_{CN} ratios were higher in Cluster 1." (lines 643–4)

L593. *Add they were still much lower than cluster 2.*

Response:

The N_{CCN}/N_{CN} ratios at 0.4–1.0% supersaturations are slightly higher in Cluster 1 than in Cluster 2. Therefore, we did not add this as a separate sentence to the main text.

L594. *Insert only after into.*

Response: "The Strait of Malacca was divided into only two clusters, both of marine origin, but associated with different source regions: the South China Sea (Cluster 1) and the Andaman Sea (Cluster 2)." (lines 645–7)

L599–601. *Just because N_{CN} is higher does not necessarily mean N_{CCN} is higher.*

Response:

Thank for pointing this out. Since various factors influence N_{CCN}, the sentence in the main text was oversimplified. Therefore, we revised the sentence as follows:

"Although the geometric mean diameter was slightly larger in Cluster 2, N_{CCN} across all supersaturations were also roughly twofold higher during the Cluster 1 period." (lines 650–2)

L608. *Insert brief before occurrence.* & **L609**. *Insert mean before N_{CN}.*

Response: "Despite the brief occurrence of the lowest N_{CN} due to intense precipitation during the Cluster 1 period, mean N_{CN} and N_{CCN} were the highest among the three clusters." (lines 659–60)

L612. *Insert only in front of from.*

Response: "Consequently, the N_{CCN}/N_{CN} ratios were lower than those of the two clusters originating only from the Indian Ocean." (lines 662–3)

L634. *Change combined to applied.*

Response: "Furthermore, clustering analysis was applied to enable a multifaceted examination of variability within individual sea areas." (lines 685–6)

L636. *Insert total before aerosol.*

Response: "Throughout the entire observation period, total aerosol (CN) and CCN number concentrations (N_{CN} and N_{CCN}) exhibited significant spatiotemporal variability, ranging from tens (or even a single digit) to several thousand per cubic centimeter." (lines 687–9)

L639. *Move a meteorological factor in front of intense precipitation. Comma after factor.*

Response: "The lowest N_{CN} and N_{CCN} occurred locally on April 9 due to a meteorological factor, intense precipitation." (lines 689–90)

L642. *Change comma to period. Delete and. Capitalize it.*

Response: "This high-concentration episode was driven by the Taal volcano located in the southern part of Luzon Island." (lines 692–3)

L643. *Change were to was. Change those to* N_{CCN}.

Response:

In response to all the referees' comments, we revised the sentence as follows.

"It was the only period during which N_{CCN} at 0.2% supersaturation (SS) was comparable to N_{CCN} at higher supersaturations." (lines 693–4)

L647. *Delete 2nd the. Change in to over.*

Response: "A similar contrast was observed in the CCN-to-aerosol (N_{CCN}/N_{CN}) ratios across the same longitude; however, higher values were observed over the Indian Ocean." (lines 697–8)

L656. *Delete 2nd the.*

Response: "This indicates that aerosols in the South China Sea were more hygroscopic and thus more readily activated into CCN than those in the Strait of Malacca, a conclusion supported by critical diameter and κ analyses." (lines 705–7)

L659. *Diameters singular.*

Response: "It was also the only region characterized by a distinct nucleation mode, resulting in the smallest geometric mean diameter among all regions." (lines 709–10)

L661. *Insert more before substantial. Change last the to a. supersaturations singular.*

Response: "Nevertheless, the Indian Ocean showed the highest κ values, indicating that the aerosols were highly hygroscopic and that a more substantial fraction of the particles could act as CCN at a given supersaturation." (lines 710–2)

L665. *Change particularly to especially.*

Response: "Since the majority of particles were in the accumulation mode and dominated by natural sulfate aerosols, N_{CCN} and their ratios were especially elevated at 0.2% SS." (lines 714–6)

L665–7. *CCN supersaturation accounts for all of these factors. Could point out that all of these factors influence CCN supersaturation.*

Response:

Thank for the referee's valuable suggestion. Taking into account that all these factors influence CCN supersaturation, we revised the sentence as follows:

"Taken together, these results demonstrate that in marine environment, various factors, such as aerosol number concentration, size distribution, and κ, plays a critical role in determining the critical supersaturation for CCN activation." (lines 716–8)

L668. *Change In the to Regarding.*

Response: "Regarding CCN spectra, the classical Twomey formula failed to adequately capture the nonlinear increase in N_{CCN} in some regions." (lines 719–20)

L672. *Insert more after be. Move variations after aerosol (singular). Delete in.*

Response: "The parameter N, representing the upper limit of N_{CCN}, was the smallest in the Indian Ocean, suggesting that cloud properties in the Indian Ocean can be more susceptible to aerosol variations." (lines 721–3)

L673–4. *Move substantially larger in front of β. Move in the South China Sea right after β. Change reflecting to reflected. Delete was. Change comma to period.*

Response: "Although the South China Sea and the Strait of Malacca exhibited similar N values, the substantially larger β in the South China Sea reflected the sensitivity of N_{CCN} to supersaturation." (lines 723–5)

L675. *Insert This is before consistent.* & **L675–6**. *Change that region to the South China Sea.*

Response: "This is consistent with the smaller critical diameters and more hygroscopic aerosols observed in the South China Sea." (lines 725–7)

L677. *Remove The.*

Response: "Clustering analysis showed that in both the East China Sea and Indian Ocean, N_{CN} and N_{CCN} were higher when air masses originated from land than from the ocean." (lines 728–9)

L678–80. *Note sea salt, NaCl.*

Response: "In contrast, the N_{CCN}/N_{CN} ratios were higher for marine-origin air masses, indicating that marine aerosols (especially sea salt such as NaCl) are more hygroscopic than continental aerosols." (lines 729–31)

[Minor Comments in Supplement]

Response:

We are also deeply pleased with the referee's comments on the supplement and once again do our best to improve it as the referee suggested.

L41. *Particularly to especially.*

Response: "The first bin was excluded because it was especially noisy and the particle size could not be reliably determined." (lines 48–9)

L43. *Comparison plural.*

Response: "For comparisons based on the mobility diameter, the aerodynamic diameters measured by the APS were converted to mobility diameters using Equation S2." (lines 50–1)

L61. *Remove in.* & **L62**. *Move except the first in front of were.*

Response: "Unlike Step 1, all APS size bins except the first were used in the fitting." (lines 68–9)

L94. *Delete to.*

Response: "In this study, since β was set to 1, a_k equals $F - 1$." (lines 100–1)

L96. *Word missing after where.*

Response: "where F represents the scaling factor for the 30-min averaged data." (line 103)

L98. *Do you mean beginning of the hour?*

Response:

The referee is correct. We averaged the data over 30-minute intervals based on the hour; for example, from 00:00 to 00:30 and from 00:30 to 01:00. To provide further clarity for the readers, we added an example in the main text.

"In this study, the data were averaged over 30-min intervals starting from the hour; for example, from 00:00 to 00:30 and from 00:30 to 01:00." (lines 105–6)

L107. *Change in to within.*

Response: "Mass concentrations were calculated by combining the SMPS and APS data to ensure consistency within the size range." (lines 114–6)

Fig. S1. *How do a & b relate? They have the same times but different plots. I do not see dashed lines. No legend in a.*

Response:

Figure S2a (originally Figure S1a) shows the aerosol size distributions for the three samples before and after the discontinuity time that is indicated in the figure title. Each set of three samples exhibits consistent distributions both before and after the discontinuity point.

Figure S2b (originally Figure S1b) shows the mean aerosol size distributions for the three samples before and after the discontinuity point presented in Figure S2a (originally Figure S1a). Although the number concentration changed by an order of magnitude, the mean size distributions remain remarkedly similar. This demonstrates the application of number concentration-based correction. We added a more detailed explanation regarding this in the main text.

"The aerosol number concentrations measured by the SMPS sometimes exhibited intermittent and discontinuous fluctuations of nearly an order of magnitude. Each set of aerosol size distributions before and after these discontinuity points were similar to others within the set (Fig. S2a). However, the non-refractory PM1 (NR-PM1) were measured by the AMS continuously at the times when there were discontinuities exhibited in the SMPS data (Fig. S3). Furthermore, when compared with CCN number concentrations, the aerosol number concentrations at low levels (corresponding to the red lines in Fig. S2a) were significantly lower than CCN number concentrations. Therefore, these SMPS samples were regarded as anomalous measurements and required correction. Meanwhile, Figure S2b shows that the mean aerosol size distributions for each set of samples before and after the discontinuity points were consistent. These results demonstrate that a constant ratio of change occurred across all size bins, suggesting that a correction based on number concentration can be justified." (lines 8–19)

Furthermore, we extensively revised Figure S2a (originally Figure S1a). We removed the right y-axis and the black scatter, which were initially included to show the consistency of the ratios across all size bins, since this is already clearly shown in Figure S2b (originally Figure S1b). Additionally, as you mentioned, the dashed lines were not clearly visible. To distinguish

the samples by color rather than line style, we changed each set of three samples before and after the discontinuity point to red and blue, respectively. The legend was also added to describe the revised figure. Other modifications include adjusting the y-axis limits in (a), swapping the left and right y-axes, and updating the number concentrations in the legend in (b). Finally, we revised the figure captions to reflect these changes.

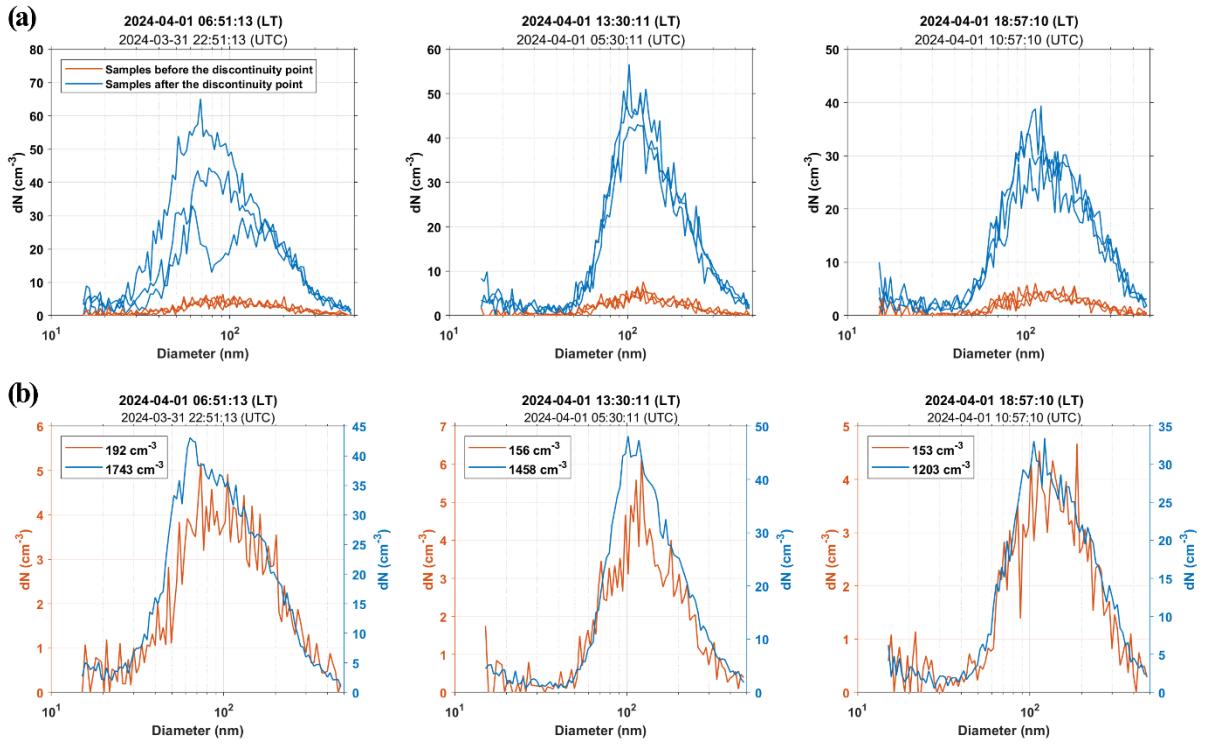

Figure S2. (a) Examples of aerosol size distributions for three samples before (red) and after (blue) the discontinuity point. (b) Mean aerosol size distributions for each set of samples before and after the discontinuity point represented in (a). The values in the legend indicate the mean aerosol number concentrations before and after the discontinuity point, respectively. The times in the titles represent the exact moment the data discontinuity occurred.

Fig. S3. *What does white line at 4 °N signify?*

Response:

We removed Figure S3 and incorporated the regional information into Figure 1.

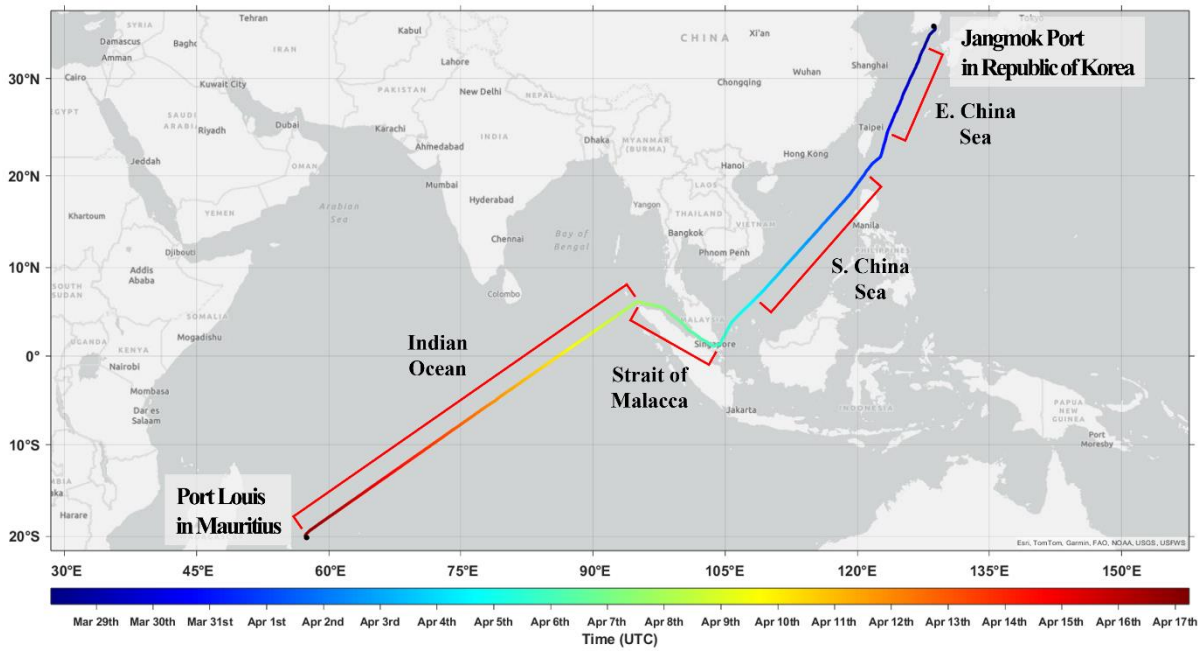

Figure 1. Cruise route of the R/V *ISABU* in 2024, including regional classification (Source: Esri, TomTom, Garmin, FAO, NOAA, USGS, USFWS; Powered by Esri).

Fig. S4, S6, and S8. *Pink lines?*

Response:

We wonder what pink lines the referee referred to. Figures S5, S8, and S11 do not include any pink lines. (Note that Fig. S4, S6 and S8 have been renumbered as Fig. S5, S8 and S11, respectively, with the addition of Fig. S1, S3, S6, and S10 and deletion of original Fig. S3)

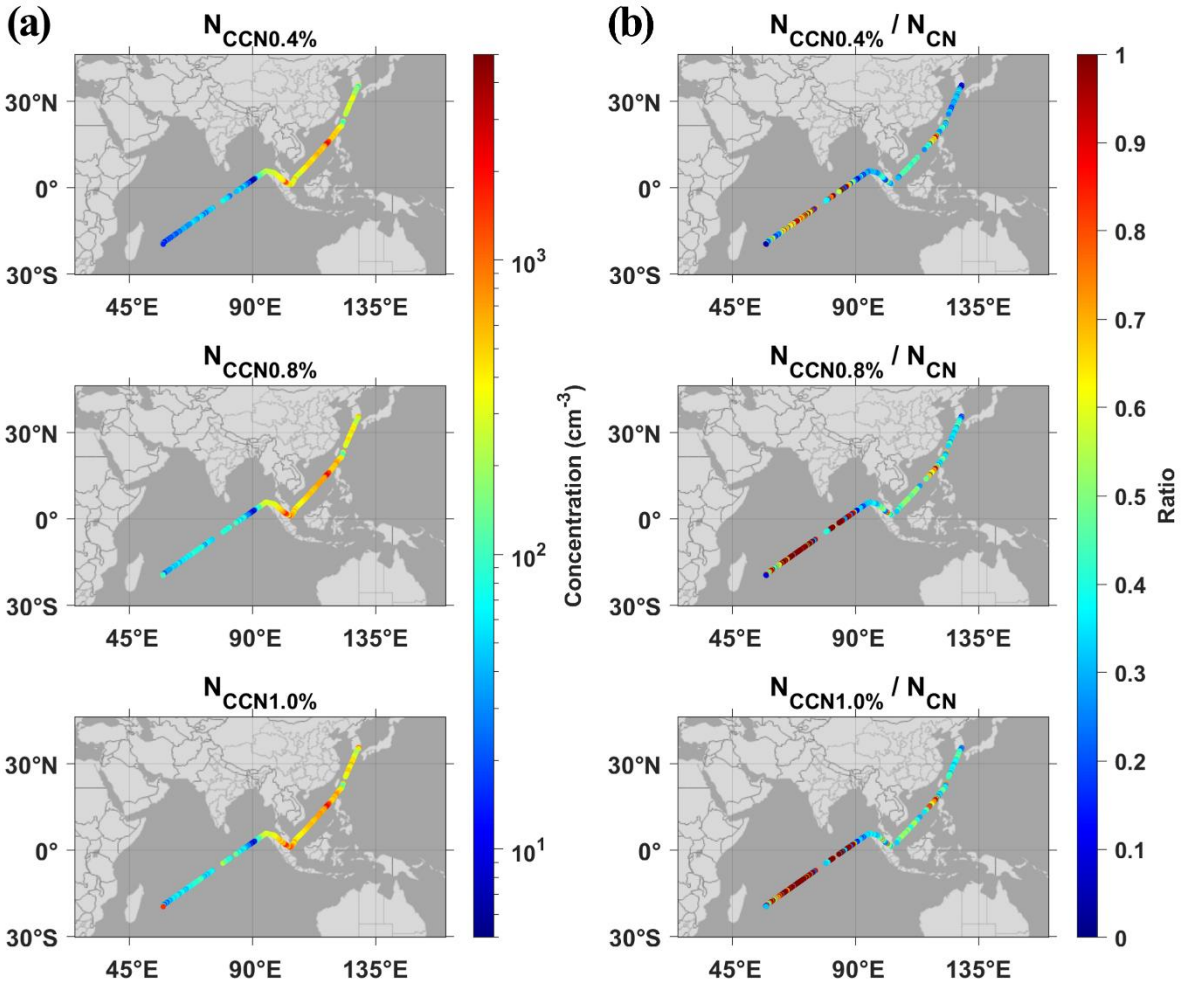

Figure S5. Spatial distributions of (a) CCN number concentrations at 0.4%, 0.8% and 1.0% supersaturation and (b) their ratios to total aerosol number concentrations during the transit voyage of the R/V *ISABU* (from Natural Earth).

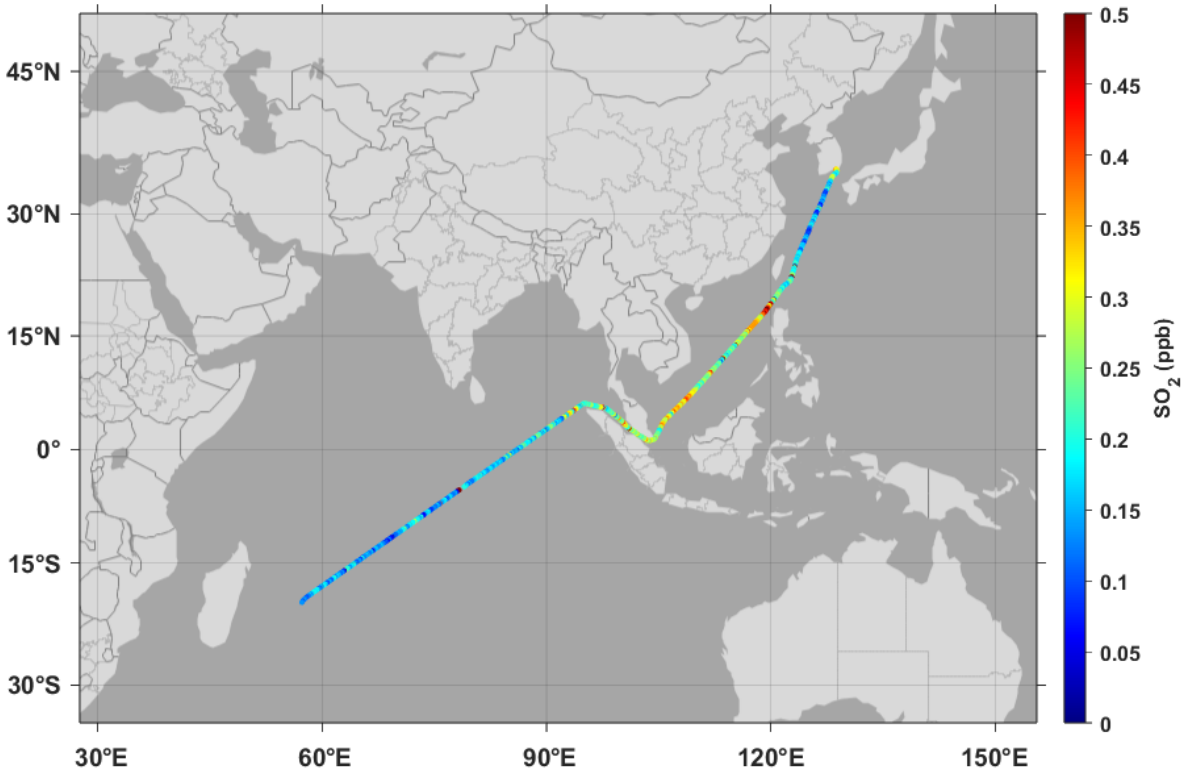

Figure S8. Spatial distribution of SO_2 measured by the Air Quality Monitoring System during the transit voyage of the R/V *ISABU* (from Natural Earth).

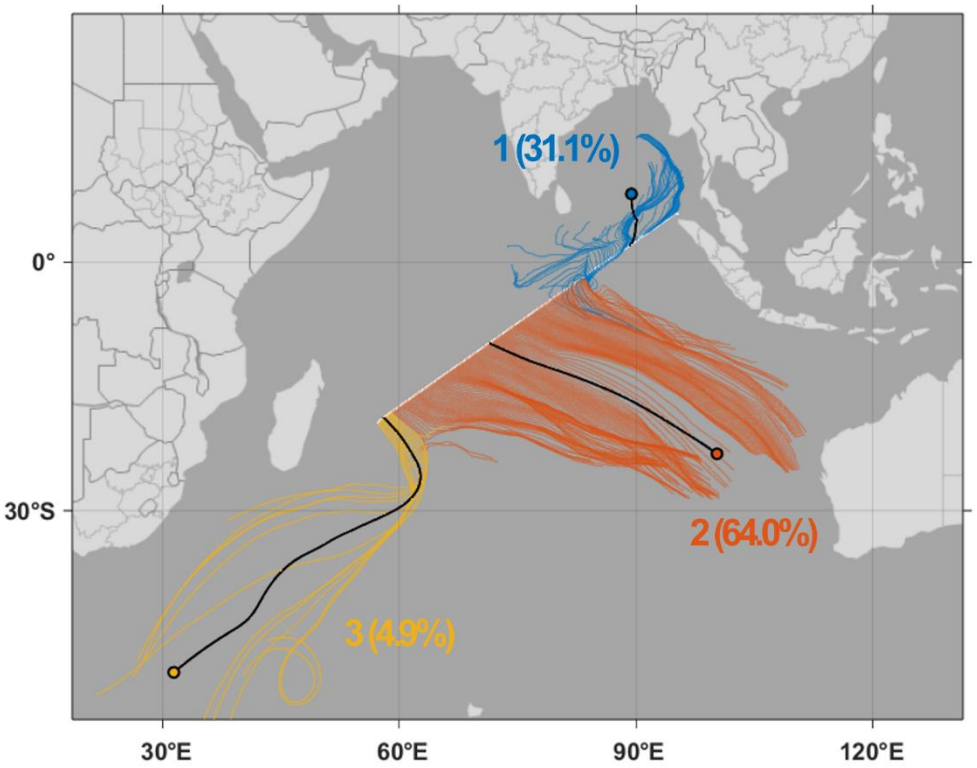

Figure S11. Results of extending each back trajectory to 120 hours in the cluster analysis for the Indian Ocean. The thick black solid lines with dots at the end represent the mean trajectories of each cluster. The percentages in parentheses indicate the proportion of trajectories assigned to each cluster. Map data from Natural Earth.

References

Atwood, S. A., Reid, J. S., Kreidenweis, S. M., Black, D. R., Jonsson, H. H., Lagrosas, N. D., Xian, P., Reid, E. A., Sessions, W. R., and Simpas, J. B.: Size-resolved aerosol and cloud condensation nuclei (CCN) properties in the remote marine South China Sea – Part 1: Observations and source classification, Atmos. Chem. Phys., 17, 1105–1123, https://doi.org/10.5194/acp-17-1105-2017, 2017.

Geng, X., Haig, J., Lin, B., Tian, C., Zhu, S., Cheng, Z., Yuan, Y., Zhang, Y., Liu, J., Zheng, M., Li, J., Zhong, G., Zhao, S., Bird, M. I., and Zhang, G.: Provenance of Aerosol Black Carbon over Northeast Indian Ocean and South China Sea and Implications for Oceanic Black Carbon Cycling, Environ. Sci. Technol., 57, 13067–13078, https://doi.org/10.1021/acs.est.3c03481, 2023.

Saputra, H., Maimun, A., and Koto, J.: Estimation and Distribution of Exhaust Ship Emission from Marine Traffic in the Straits of Malacca and Singapore using Automatic Identification System (AIS) Data, J. Mek., 36, 86–104, available at: https://jurnalmekanikal.utm.my/index.php/jurnalmekanikal/article/view/58 (last access: 4 April 2026), 2013.

Ou, H., Cai, M., Zhang, Y., Ni, X., Liang, B., Sun, Q., Mai, S., Sun, C., Zhou, S., Wang, H., Sun, J., and Zhao, J.: Measurement report: Cloud condensation nuclei (CCN) activity in the South China Sea from shipborne observations during the summer and winter of 2021 – seasonal variation and anthropogenic influence, Atmos. Chem. Phys., 25, 2495–2513, https://doi.org/10.5194/acp-25-2495-2025, 2025.

Wilks, D. S.: Statistical Methods in the Atmospheric Sciences, 3rd edn., International Geophysics Series, Vol. 100, Academic Press, Oxford, 676 pp., ISBN 9780123850225, 2011.

Response to Anonymous Referee #2

Referee #2

This study presents continuous ship-based observations of marine aerosols and CCN across multiple oceanic regions, providing a comprehensive comparison of aerosol and CCN characteristics using a consistent analytical framework.

I appreciate that this study provides observations and direct comparisons across multiple regions, conducted across diverse sea areas using a consistent framework. This is a clear strength of the manuscript. Overall, the paper is also very well written and grammatically sound. The key conclusions of this manuscript are likely valid; however, I recommend that the authors provide stronger justification and quantitative support to demonstrate the robustness of their results. Several aspects of the analysis currently lack sufficient methodological detail and uncertainty assessment, which makes it difficult to fully evaluate the strength of the conclusions. My specific comments are provided below.

Importantly, the modal fitting presented in the manuscript requires substantial revision. The current fits do not adequately represent the measured size distributions and undermine the interpretation of modal contributions. This issue should be addressed prior to publication.

Response:

We greatly appreciate the referee for taking precious time in providing the detailed and constructive comments. We tried our best to carefully account for all comments from the referee that will certainly improve the manuscript and supplement. We hope that the revised manuscript and supplement meet the standards of the referee. Basically, responses are provided with detailed explanations for each comment and all modifications in the main text are highlighted in blue.

[Comments 1] – Paragraph 1

The opening paragraph frames the study in terms of aerosol radiative forcing and its role in the Earth's energy balance, including detailed discussions of IPCC AR6 forcing estimates and comparison to CO_2. This initially suggests that the manuscript will focus on aerosol radiative impacts. However, the study is instead centered on CCN activity and process-level aerosol-cloud interactions. This creates a disconnect between the introduction and the actual scope of the work. I recommend revising the opening paragraph to better align with the study objectives by reducing the emphasis on radiative forcing and instead focusing more directly on CCN-

relevant processes and uncertainties.

Response:

Thank for the referee's insightful suggestions. We reduced the sentences regarding radiative forcing and instead focused more on aerosol–cloud interactions and their associated uncertainties.

"Atmospheric aerosols play a critical role in cloud formation and evolution by acting cloud condensation nuclei (CCN), thereby influencing cloud droplet concentration and size, albedo, cloud lifetime, and precipitation efficiency (Twomey, 1974; Albrecht, 1989). Therefore, aerosol–cloud interactions are recognized as one of the largest sources of uncertainty in climate prediction, particularly over marine regions where extensive low-level clouds are highly sensitive to aerosol perturbations (Carslaw et al., 2013; Bellouin et al., 2020; Forster et al., 2021; Chen et al., 2024). Despite their importance, substantial uncertainties remain in understanding how aerosol characteristics control CCN activity and cloud responses across different marine environments. Improving our understanding of the factors governing CCN activation is thus essential for reducing uncertainties in aerosol–cloud interactions." (lines 34–43)

[Comments 2] – Paragraph 2

The introduction provides a limited and somewhat unbalanced overview of marine aerosol sources, and is not well aligned with the scope of the study. For example, while sulfate formation from DMS is discussed, the role of DMS-derived secondary organic aerosol is not considered, and marine organics are only attributed to primary sea spray emissions. More broadly, as no aerosol composition measurements are presented, the source-focused discussion reads more like that of a source apportionment study than one centered on CCN activity and κ*. I recommend revising this section to focus more directly on factors controlling hygroscopicity and CCN activation (e.g., particle size, mixing state, and general compositional influences), rather than detailed source attribution that cannot be constrained by the measurements in this work.*

Response:

In accordance with the referee's valuable comment, we removed most of the sentences related to marine aerosol sources from second paragraph. Furthermore, to better focus on the factors governing aerosol hygroscopicity and activation behavior, we merged the second and third paragraphs and revised them as follows.

"The ability of aerosols to act as CCN is mainly governed by their size, and secondarily by their chemical composition and mixing state (Dusek et al., 2006). Together, these factors determine aerosols hygroscopicity (κ) and, ultimately, activation behavior. Larger particles are more likely to activate at lower supersaturations due to smaller curvature effect, while aerosol composition affects the critical supersaturation required for activation according to their κ (Petters and Kreidenweis, 2007). For example, sea-salt-dominated environments typically exhibit large particles with high κ, facilitating efficient CCN activation (King et al., 2012; Gaston et al., 2018). Sulfate-rich aerosols, though generally smaller than sea salt, also contribute to CCN due to their high κ (Sanchez et al., 2018; Park et al., 2021). In contrast, increased contributions from organic aerosols can substantially reduce κ and induce large variations in CCN number concentrations (N_{CCN}) depending on their relative abundance (Martin et al., 2011; Coggon et al., 2014). As such, even modest changes in marine aerosol characteristics can significantly alter CCN activity, ultimately modifying the properties of marine low-level clouds like stratocumulus and shallow cumulus clouds (Wood et al., 2015; Fan et al., 2016). Therefore, aerosol–cloud interactions over the ocean remain a key contributor to climate prediction uncertainty, underscoring the need for long-term, spatially extensive observations of aerosols and CCN." (lines 44–60)

[Comments 3] – Paragraph 4 and 5

A summary table of the previous studies discussed in the introduction would be helpful. Consider including columns for location, N_{CN}, N_{CCN}, and N_{CCN}/N_{CN} ratio to facilitate comparison with the results presented in this study.

Response:

Following the referee's suggestion, we added a table in the main text that summarizes the previous studies mentioned in the introduction.

Table 1. Mean aerosol and CCN number concentrations (N_{CN} and N_{CCN}), critical diameter (D_C), and hygroscopicity (κ) across various marine regions in this study and previous studies.

Observation Site	Group	Period	N_{CN} (cm^{-3})	N_{CCN} (cm^{-3})	D_C (nm)	κ	Reference
Northern Hemisphere							
Arctic	Marine air mass	Sep 18–28, 2017	414±452	35±40	103±43	–	Park et al. (2020)
	Terrestrial air mass		1396±1279	71±47	83±18	–	
Pacific	Marine air mass	Aug 28–Sep 16, 2017	384±86	204±86	136±67	–	
Bohai Sea and Yellow Sea		Dec 9–19, 2019	11000±7200	2000±1300	–	0.22[a]	Gong et al. (2023)
	include East China Sea	Dec 28, 2019–Jan 16, 2020	5200±3200	1200±750	–	0.36[a]	
South China Sea		May 5–Jun 9, 2021	6966±9249	4392±6415	57±9	0.54±0.21	Ou et al. (2025)
		Dec 19–29, 2021	4988±3474	2218±1503	79±8	0.19±0.05	
Northen Indian Ocean	Southeastern Arabian Sea 1	Jan 16–Fab 13, 2018	9256±8516	3456±876	98±17	0.13±0.12	Nair et al. (2020)
	Southeastern Arabian Sea 2		2963±684	2236±453	77±9	0.22±0.04	
	Southeastern Arabian Sea 3		4251±3699	1973±391	95±36	0.15±0.08	
	Equatorial Indian Ocean		3080±3548	722±298	87±15		

(continue)

Southern Hemisphere							
Southwestern Indian Ocean		13 Jan – 8 Mar 2021 1 Jul – 22 Jul 2021 13 Sep – 3 Oct 2021 28 Oct – 28 Nov 2021 28 Nov – 30 Dec 2021 18 Jan – 24 Feb 2023	1149±706	208±102	80±15	0.2±0.1	Dournaux et al. (2025)
Southern Ocean (Australian Sector)		15 Jan – 24 Feb 2018	540±246	123±58	–	–	Sanchez et al. (2021)[b] (0.3% SS)
Antarctic	Leg 1	20 Dec 2016 – 19 Jan 2017	390	134	73	0.36	Tatzelt et al. (2022) (0.3% SS)
	Leg 2	22 Jan – 22 Fab 2017	277	143	64	0.63	
	Leg 3	26 Feb – 19 Mar 2017	319	116	67	0.55	
East China Sea		Mar 28–Apr 17, 2017	1039±451	280±67	140±22	0.05±0.02	This study
South China Sea			1226±517	538±73	112±24	0.12±0.15	
Strait of Malacca			1449±1050	441±249	155±36	0.05±0.07	
Indian Ocean			148±229	54±54	124±74	0.32±0.29	

Note: Note: The size ranges for N_{CN} vary across the previous studies. N_{CCN}, D_C, and κ values are presented at 0.4% SS for consistency. If the values at 0.4% SS were unavailable, values at the closest supersaturation are provided and the corresponding supersaturation is indicated in the reference column.

a: Mean values calculated by excluding values below 0.1.

b: While both ship and aircraft measurements were conducted in this study, only statistical values for the aircraft measurements were

[Comments 4] – Lines 198–200

Please quantify how much data (%) was excluded based on the relative wind direction filtering used to avoid ship exhaust contamination. This will help assess the representativeness of the remaining dataset.

Response:

Through relative wind direction filtering, approximately 2.8% of the data were considered contaminated by the vessel's exhaust and were excluded from this study. We added this information to the main text.

"Fortunately, the wind blew from the bow during most of the cruise (Fig. 2b), and contamination by exhaust was minimal at 2.8%." (lines 183–185)

[Comments 5] – Lines 212–213

I find it problematic that AMS mass is used to "validate" SMPS/APS-derived mass, as the typical approach is the reverse. SMPS measurements are used to constrain AMS mass via collection efficiency and subsequent scaling. As presented, there is insufficient methodological detail to evaluate this comparison. For example, was size-dependent transmission efficiency accounted for? Additionally, how were refractory components treated in the mass comparison, given that the AMS measures only non-refractory species?

Response:

We appreciate the referee's insightful comments regarding the comparison between SMPS/APS and AMS data. We agree that AMS mass concentrations should not be used as a quantitative validation standard for mass concentrations derived from SMPS/APS number size distribution. That is because AMS inherently cannot detect refractory components such as sea salt, mineral dust, and black carbon, although we partially accounted for the size-dependent transmission efficiency of the AMS. Accordingly, we revised the manuscript and supplement to ensure that the AMS data is no longer presented as a quantitative validation standard for the SMPS correction.

First, in the revised manuscript, we solely utilized $PM_{2.5}$ data measured by the beta attenuation method for the validation of SMPS corrections. This data provides a more appropriate reference for the total particle mass compared to the NR-PM1 from the AMS. Accordingly, we specified that the validation was performed exclusively against $PM_{2.5}$ data, and Figure S4 is modified to display only the $PM_{2.5}$ comparisons.

"The corrected data were then validated against the $PM_{2.5}$ data obtained by the beta attenuation method before being used for this study (Fig. S4)." (lines 199–200 in manuscript)

"These results were compared with $PM_{2.5}$ data based on the beta attenuation method." (lines 113–114 in supplement)

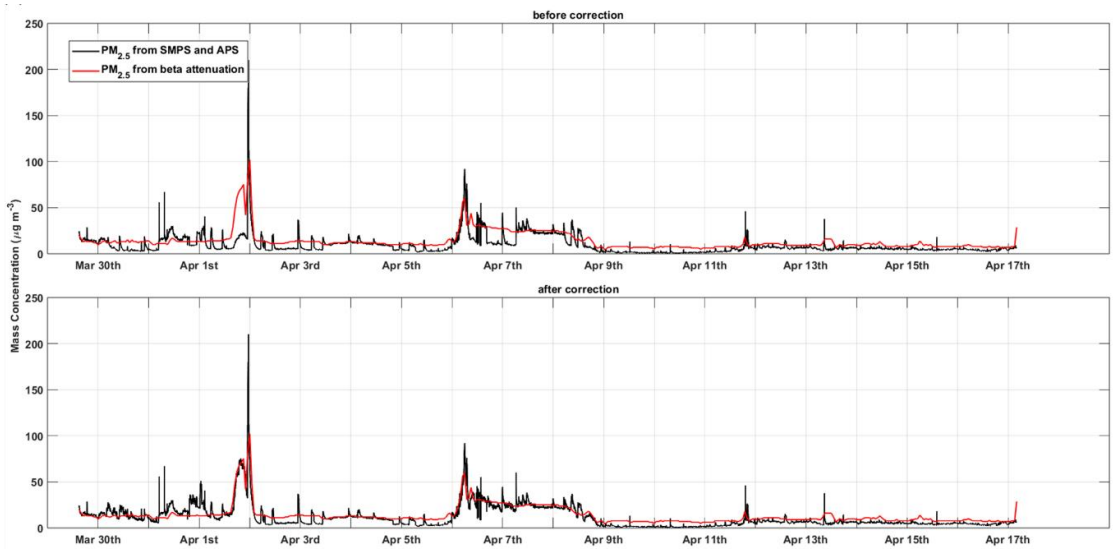

Figure S4. Comparison of mass concentrations of particles smaller than $2.5\ \mu m$ before (top) and after (bottom) the number concentration correction of SMPS. The black and red lines represent $PM_{2.5}$ calculated by combining SMPS and APS data and $PM_{2.5}$ measured using the beta attenuation method, respectively.

Meanwhile, the AMS data were used only supplementarily for qualitative verification of temporal consistency. Specifically, if the variations in SMPS number concentrations, which spanned nearly an order-of-magnitude, reflected real atmospheric changes, a corresponding change would be also expected in the NR-PM1 time series from the AMS. However, the NR-PM1 times series showed continuous and smooth variation at the points where discontinuities were exhibited in the SMPS data. This finding is interpreted as evidence that the discontinuities of SMPS were anomalous changes caused by instrument malfunction rather than actual atmospheric fluctuations. Therefore, separately from Figure S4, we added a new figure (Fig. S3) showing the time series of the total aerosol number concentration before the SMPS corrections alongside the NR-PM1 measured by the AMS. A brief explanation of this is also incorporated into the main text.

"If these variations reflected real atmospheric changes, they should be clearly evident in the non-refractory PM1 data measured by the Aerosol Mass Spectrometer. However, since no such signal was observed, the SMPS data are presumed to be anomalous." (lines 194–197 in manuscript)

"However, the time series of non-refractory PM1 (NR-PM1) measured by the AMS remained continuous at the times when discontinuities exhibited in the SMPS data (Fig. S3)." (lines 11–12 in supplement)

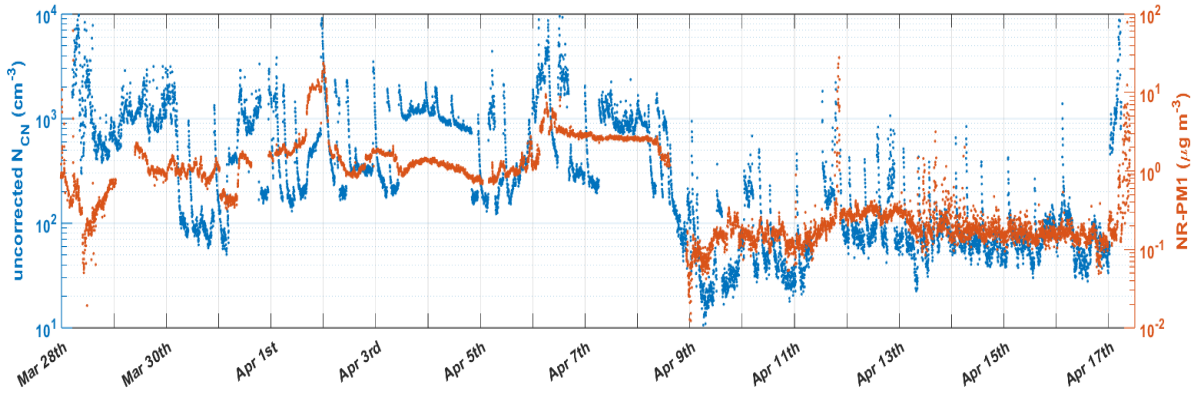

Figure S3. Time series of (left) total aerosol number concentrations before the correction of SMPS and (right) NR-PM1 measured by the AMS.

[Comments 6] – Lines 276

I initially assumed that the Aitken and accumulation modes were derived from fitted SMPS size distributions; however, this was only clarified upon reading the Figure 5 caption. The size ranges used to define the nucleation, Aitken, and accumulation modes should be explicitly stated in the main text, preferably within the Methods section.

Response:

Thank for pointing out this important point. As suggested, we added the definitions for the three modes to Section 2.1.2.

"In addition, to investigate the size-resolved variations of aerosols, we categorized the SMPS size range into three modes: nucleation mode (15–25 nm), Aitken mode (25–100 nm), and accumulation mode (100–478.3 nm)." (lines 153–155)

[Comments 7] – Lines 291

Change "were similar to those at the other supersaturations." to "were similar to N_{CCN} at the other supersaturation."

Response:

In response to all the referees' comments, we revised the sentence as follows.

"A crucial point is that this period was the only instance in which the N_{CCN} at 0.2% SS, where only relatively large aerosols can activate, were similar to N_{CCN} at the other supersaturations (Fig. 3b)." (lines 303–306)

[Comments 8] – Lines 299–300

Is this conclusion based on the range of measured values? Please quantify the difference to make this statement clear.

Response:

Yes, this conclusion is based on our measurement data. To support this statement, we included specific quantitative values in the main text.

"However, the distribution of the geometric mean diameter was larger when exiting the strait (85.6 ± 17.2 nm when entering vs. 113.5 ± 17.7 nm when exiting)." (lines 315–316)

[Comments 9] – Lines 300–301

Be explicit about mode number concentrations in text.

Response:

Similar to the point raised in Comment 8, we added the ratio of Aitken mode to accumulation mode to this statement. Furthermore, we reviewed other statements throughout the main text to ensure that they are supported by quantitative values.

"This is because the ratio of Aitken mode to accumulation mode was lower upon exiting the strait (1.32 ± 0.80 when entering vs. 0.49 ± 0.20 when exiting)." (lines 316–318)

"N_{CN} were higher upon entering the strait from the South China Sea than upon exiting into the Indian Ocean (2153 ± 1257 cm^{-3} when entering vs. 901 ± 212 cm^{-3} when exiting)." (lines 310–312)

"N_{CCN} at 0.2% SS exhibited a relatively uniform concentration within the strait, whereas N_{CCN} at the other supersaturations were higher upon entering the strait (at 0.6% SS, 753 ± 404 cm^{-3} when entering vs. 332 ± 57 cm^{-3} when exiting), consistent with the pattern of N_{CN}." (lines 318–321)

"Over the Indian Ocean, on April 9 (UTC), N_{CN} and N_{CCN} decreased sharply, reaching their minimum values (N_{CN}: 11 cm^{-3}; N_{CCN} at 0.2 and 0.6% SS: 1 and 3 cm^{-3}, respectively) during the cruise." (lines 323–325)

[Comments 10] – Lines 305–311

Please quantify the difference between N_{CN} and N_{CCN} during non-precipitation periods over the Indian Ocean. Additionally, indicate what fraction of the dataset (%) is affected. Consider excluding precipitation events in the comparisons to other regions.

Response:

Following the comment, we examined the N_{CN} and N_{CCN} during non-precipitating periods over the Indian Ocean, as well as during precipitating periods for a comprehensive comparison. The results are added into the manuscript as follows.

"Meanwhile, in the Indian Ocean, N_{CN} and N_{CCN} (at 0.2% and 0.6% SS) during non-precipitating periods were 150, 30, and 67 cm^{-3}, respectively, which were higher than the average values during the precipitating periods (130, 11, and 37 cm^{-3}). However, the difference between N_{CN} and N_{CCN} was similar across both periods." (lines 328–332)

Furthermore, in Section 3.2, we performed a re-analysis excluding precipitation periods to ensure a more consistent comparison across the various regions. While precipitation occurred during 2.55% of the entire voyage, this figure reduces to 1.44% (0.05% in the Strait of Malacca and 1.39% in the Indian Ocean) when excluding periods that were not classified

into any specific maritime region (e.g., March 28th). As the duration of precipitation was minimal, the results remained largely unchanged. Therefore, we updated the quantitative values in the main text (including Tables 2 and 3) and remade the figures, while the original narrative remains unchanged. We also added a statement clarifying the exclusion of precipitation periods at the beginning of Section 3.2.

"Additionally, to ensure a consistent comparison, periods affected by precipitation—accounting for 1.44% of the period classified into specific marine regions (0.05% in the Strait of Malacca and 1.39% in the Indian Ocean)—were excluded from the analysis." (lines 403–406)

[Comments 11] – Lines 410–418

This values reported for the South China Sea and the Strait of Malacca appear quite comparable. For example, the difference in N_{CN} (1226 vs. 1446 cm^{-3}) is likely within measurement uncertainty, and a similar overlap is evident for NCCN at both supersaturations. With error propagation, the N_{CCN}/N_{CN} ratios are even more likely to fall within measurement uncertainty. I recommend including uncertainty estimates in your analysis to assess whether these differences are robust enough to support the conclusions drawn.

Response:

We thank the referee for this important comment. Following the referee's suggestion, we quantified the measurement uncertainties of both N_{CN} and N_{CCN} and assessed their propagation into the N_{CCN}/N_{CN} ratio. In this analysis, the measurement uncertainties for N_{CN} and N_{CCN} were assumed to be 10% and 4%, respectively, following Wiedensohler et al. (2018) and Uin and Enekwizu (2024). Based on standard error propagation, the relative uncertainty in the N_{CCN}/N_{CN} ratio is estimated to be 10.8%. Accordingly, the mean N_{CCN}/N_{CN} ratios and their absolute uncertainties at 0.2% and 0.6% SS are 0.23 ± 0.025 and 0.51 ± 0.055 for the South China Sea, and 0.19 ± 0.021 and 0.39 ± 0.042 for the Strait of Malacca, respectively (Table S2). We included these uncertainty estimates in the manuscript and added a summary table in the supplement.

"However, when accounting for measurement uncertainties, the ranges of both ratios at 0.2% SS overlap slightly, whereas at 0.6% SS, they remain distinct without overlap (Table S2)." (lines 443–445)

Table S2. Ratios of CCN number concentration to total aerosol number concentration (N_{CCN}/N_{CN}) and measurement uncertainties by supersaturation in the South China Sea and the Strait of Malacca.

	South China Sea		Strait of Malacca	
SS (%)	N_{CCN}/N_{CN} ratio	Uncertainty	N_{CCN}/N_{CN} ratio	Uncertainty
0.2	0.23	0.025	0.19	0.021
0.4	0.49	0.053	0.34	0.037
0.6	0.51	0.055	0.39	0.042
0.8	0.52	0.056	0.43	0.046
1.0	0.52	0.056	0.44	0.048

Note. Measurement uncertainties for N_{CN} and N_{CCN} are assumed to be 10% and 4%, respectively, following Wiedensohler et al. (2018) and Uin and Enekwizu (2024). Based on the standard error propagation, the relative uncertainty for N_{CCN}/N_{CN} is 10.8%, and the corresponding absolute uncertainties are presented in the table.

[Comments 12] – Section 3.2.2.

The modal fits shown here are not convincing and do not adequately reproduce the measured size distributions. In particular, the accumulation mode peak height is consistently underestimated (e.g., in the East China Sea, South China Sea, and Strait of Malacca), while the peak with appears overestimated to compensate, resulting in poor representation of the observed distributions. This suggests that the fits are not well constrained and may not reflect a physically meaningful decomposition. Some residual analysis should be presented.

In addition, modal fitting was not described in the Methods section prior to this discussion, making it difficult to assess how these fits were performed or constrained. Since the SMPS data were merged with APS measurements, the modal fitting should be performed on the merged size distribution to properly capture the full accumulation mode, particularly the coarse-mode shoulder. Fitting only a subset of the size range likely contributes to the systematic underestimation of the accumulation mode peak and misrepresentation of its width.

Finally, these distributions should be presented using a lognormal y-axis scaling (e.g.,

consistent with dN/dlogDp representation) to properly evaluate the quality of the fits and the relative contributions of each mode.

Response:

We sincerely appreciate the referee's important comment regarding the modal fitting. As the fitting was performed using only the SMPS data, the coarse-mode shoulder was not properly captured, which led to an underestimation of the accumulation mode. To address this issue, we conducted a new modal fitting on the merged size distribution ranging from 15 to 3000 nm using the APS data. We also refined the physical interpretation based on the new results.

"The nucleation mode was carefully interpreted, as it was fitted within a significantly restricted geometric mean diameter range (15–25 nm) to account for occasional voltage instabilities in the smallest size bins of the SMPS.

Submicron aerosols dominated the total number concentrations across all regions. In contrast, while the contribution of the coarse mode to the number concentrations was minor, these particles could play a substantial role in CCN activation at low supersaturations.

In the East China Sea, South China Sea, and Strait of Malacca, three submicron modes were observed, but the distributions were characterized by prominent Aitken and accumulation modes." (lines 483–491)

"In contrast, the Indian Ocean exhibited much lower number concentrations across all three submicron modes, but a relatively distinct separation among these modes." (lines 500–501)

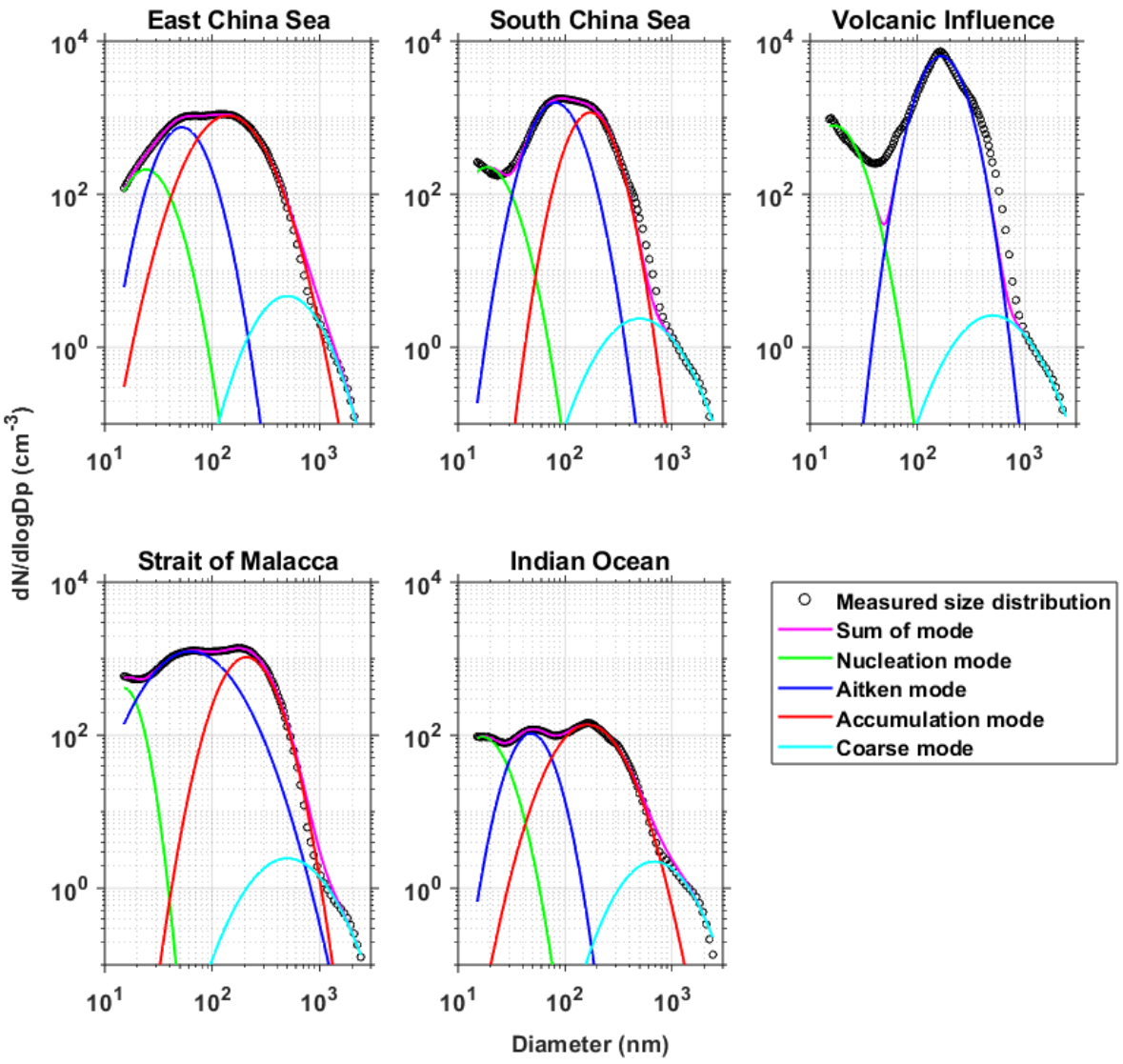

Figure 9. Average aerosol size distributions (black circles) for each sea area along with the fitting results for each mode (green, blue, red, and cyan lines). The distribution for the sum of all modes is represented by a magenta line. For the South China Sea, the volcanic-influence period was depicted separately.

To enhance consistency and reproducibility in the modal fitting, we modified our methodology and added detailed descriptions of the updated method to the Methods section in the manuscript. Furthermore, following the referee's suggestion, we included information on residuals along with the fitting parameters in the supplement (Table S3). We also presented the reasons for the poor fitting performance during the volcanic-influence period based on a residual analysis.

"*2.2.2. Fitting of multiple lognormal modes*

Merged SMPS–APS size distributions (15–3000 nm) were fitted with multiple lognormal modes to characterize the aerosol modal structure, where each mode was expressed as follows:

$$N_i(D_p) = \frac{N_{t,i}}{\sqrt{2\pi}\log_{10}\sigma_{g,i}} exp\left[\frac{-(\log_{10}D_p - \log_{10}D_{pg,i})^2}{2(\log_{10}\sigma_{g,i})^2}\right], \quad (1)$$

where D_p denotes the aerosol diameter. $N_{t,i}$, $D_{g,i}$ and $\sigma_{g,i}$ are the total number concentrations, the geometric mean diameter, and the geometric standard deviation of mode i, respectively.

To better reproduce the broad large-particle shoulder, following the concept of Modini et al. (2015), the coarse mode was first fitted to the upper part of the size distribution (1000–2500 nm) using a constrained single lognormal mode, with bounds of $N_t = 0 - 20\ cm^{-3}$, $D_{pg} = 500 - 1800\ nm$ and $\sigma_g = 1.5 - 3.0$. These bounds were selected to allow a single broad mode to represent the observed coarse mode shoulder while minimizing interference from the dominant submicron modes. In addition, while the upper limit of the merged size distribution is 3000 nm, the coarse mode fitting was only performed up to 2500 nm to avoid overfitting in the 2500–3000 nm range, where number concentrations were negligible.

The fitted coarse mode was then subtracted, and the residual submicron distribution (15–1000 nm) was fitted with multiple lognormal modes. The maximum number of submicron modes was limited to three to preserve physically interpretable mode structures. The optimal number of modes was determined sequentially: when the addition of one extra mode decreased the RMSE by less than 10%, the previous number of modes selected as optimal. The parameter bounds for the submicron modes were basically $D_{pg} = 15 - 25\ nm$ and $\sigma_g = 1.0 - 1.5$ for the nucleation mode, $D_{pg} = 25 - 100\ nm$ and $\sigma_g = 1.0 - 2.0$ for the Aitken mode, and $D_{pg} = 100 - 500\ nm$ and $\sigma_g = 1.0 - 2.0$ for accumulation mode, with $N_t = 0 - 10000\ cm^{-3}$ for all three." (lines 212–234)

"Finally, based on the residuals, the performance of the fitting for the volcanic-influence period was relatively poor compared with the other four regions (Table S3). Although four submicron peaks were identified in the measured size distribution (< 40, ~70, ~170, and ~400 nm), increasing the number of submicron modes from two to three reduced the RMSE by less than 10%. Consequently, only the nucleation and accumulation modes were ultimately fitted, resulting in substantial underestimation at around 50 nm and 600 nm (Fig. S10). Nevertheless, it is evident that a distinct accumulation mode ($N_t = 2468\ cm^{-3}$, $\sigma_g = 1.43$) was observed during the volcanic-influence period." (lines 508–515)

Table S3. Summary of fitting parameters and residuals for the lognormal modal fitting in each sea area.

	East China Sea			South China Sea			Strait of Malacca			Indian Ocean			Volcanic Influence		
Fitting parameter															
	N_t	D_{pg}	σ_g	N_t	D_{pg}	σ_g	N_t	D_{pg}	σ_g	N_t	D_{pg}	σ_g	N_t	D_{pg}	σ_g
Nucleation	92.67	24.10	1.50	99.09	18.68	1.50	123.79	15.00	1.32	41.79	16.91	1.50	348.53	16.61	1.50
Aitken	325.39	52.12	1.49	675.62	80.97	1.48	922.87	62.80	1.98	41.38	48.05	1.44	–	–	–
Accumulation	636.96	139.98	1.74	474.98	171.82	1.45	489.72	207.60	1.54	81.74	162.80	1.73	2467.84	165.91	1.43
Coarse	2.71	500.00	1.71	1.63	500	1.88	1.74	500	1.92	1.44	681.24	1.81	1.79	500	1.89
Residuals															
RMSE	4.6953			21.6569			299.9474			8.8404			2.3919		
NRMSE	0.0042			0.0121			0.041			0.0064			0.0166		
MBE	0.5855			–3.3388			–52.4177			0.5868			0.0502		
MARR (15–25)	1.44			14.81			17.31			2.26			1.08		
MARR (25–100)	0.33			4.79			45.36			0.55			0.47		
MARR (100–500)	1.71			9.04			25.25			1.15			3.87		

Note. RMSE and NRMSE are the root-mean-square error and normalized root-mean-square error, respectively. MBE denotes the mean bias error, and MARR denotes the mean absolute relative residual (%).

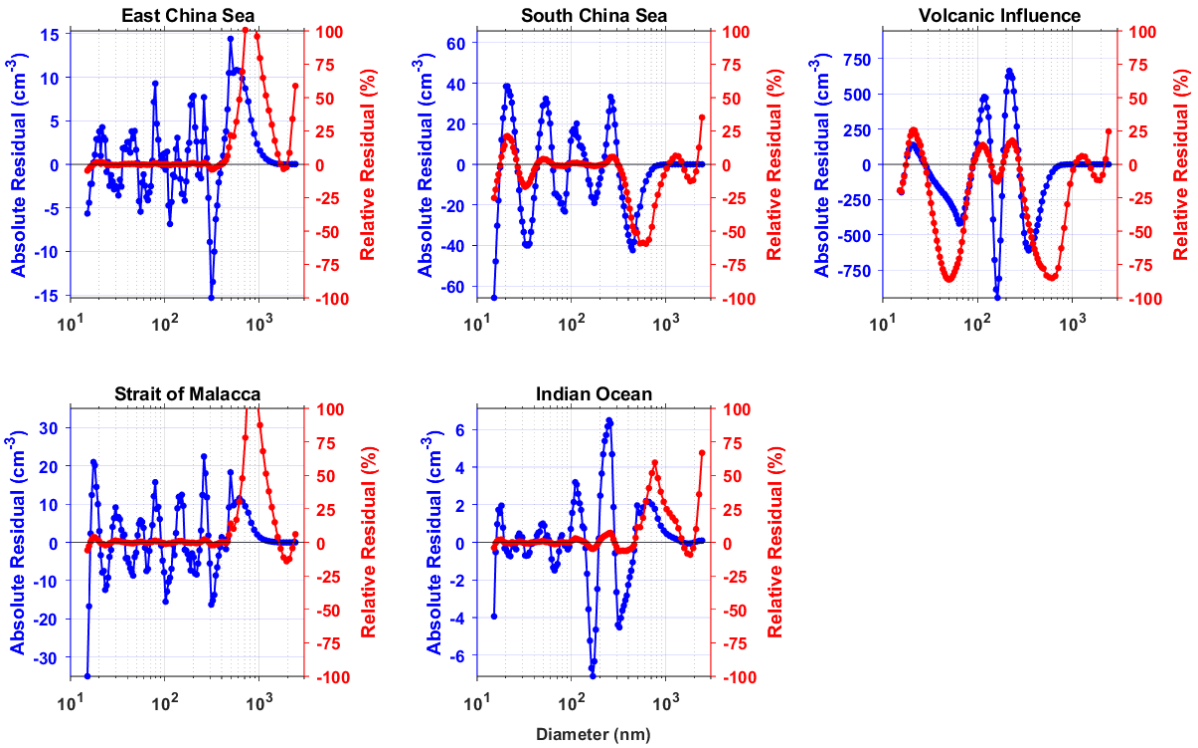

Figure S10. Size-dependent absolute (blue) and relative (red) residuals for the lognormal modal fitting in each sea area.

[Comments 13] – Lines 409

The use of "dominance" is unclear in this context. It is not evident whether this refers to sulfate representing the largest mass fraction of the aerosol or to sulfate disproportionately controlling hygroscopicity. Additionally, as this interpretation appears to be based on SO_2 concentrations rather than direct composition measurements, the statement is too definitive. I suggest revising the wording to indicate that sulfate is likely an important contributor, rather than asserting dominance, unless further evidence can be provided.

Response:

We thank the referee for this thoughtful comment. Indeed, we agree that we should not be too definitive. Following the referee's suggestion, we revised the sentence using a more tentative tone.

"Meanwhile, the N_{CCN}/N_{CN} ratios at 0.2% SS during the volcanic-influence period were exceptionally high, which was likely due to contribution of hygroscopic sulfate aerosols in addition to the largest aerosol sizes." (lines 434–436)

[Comments 14] – Lines 481

Please quantify the measurement uncertainties (%) at each supersaturation in a Table (in the supplement should suffice).

Response:

According to the manufacturer's manual, at low supersaturation (e.g., <0.2%), the maximum CCN count rate decreases at higher particle concentrations due to counting limitations such as coincidence effects in the optical particle counter.

In addition, Rose et al. (2008), which systematically investigated the calibration and measurement uncertainties of the DMT-CCNC, reported that the uncertainty in effective supersaturation becomes substantially larger at low supersaturation (≤0.1%). This is because the relationship between the column temperature gradient and supersaturation is non-linear at low supersaturation.

Nevertheless, it is difficult to assign a single quantitative uncertainty value for CCN concentrations at each supersaturation, as the overall uncertainty depends on multiple factors, including supersaturation calibration accuracy, OPC counting efficiency, the slope of the activation curve, and aerosol number concentrations.

[Comments 15] – Lines 585–586

This statement is too definitive given that no direct compositional measurements are presented. If this interpretation is based on SO_2 or other indirect proxies, the language should be softened. I recommend revising to indicate that sulfate is likely an important contributor, rather than asserting a substantial fraction, unless additional supporting evidence is provided.

Response:

Thank for the suggestion. But, instead of softening the tone in this sentence, we removed the reference to sulfate.

"Moreover, N_{CCN} during the Cluster 2 period were at least twice N_{CCN} observed in Clusters 1 and 3, with the difference being particularly evident at 0.2% SS." (lines 637–638)

[Comments 16] – Lines 634

Change "clustering analysis was combined to enable a" to "clustering analysis enabled".

Response:

In response to all the referees' comments, we revised the sentence as follows.

"Furthermore, clustering analysis was applied to enable a multifaceted examination of variability within individual sea areas." (lines 685–686)

[Comments 17] – Lines 643

Change "were closed to those at higher supersaturation." to "were comparable to N_{CCN} at higher supersaturations."

Response:

This sentence is also revised as follows, incorporating all the referees' comments.

"It was the only period during which N_{CCN} at 0.2% supersaturation (SS) was comparable to N_{CCN} at higher supersaturations." (lines 693–694)

[Comments 18] – Figure 1

This can be in the supplement.

Response:

Following the suggestion, Figure 1 is moved from the manuscript to the supplement.

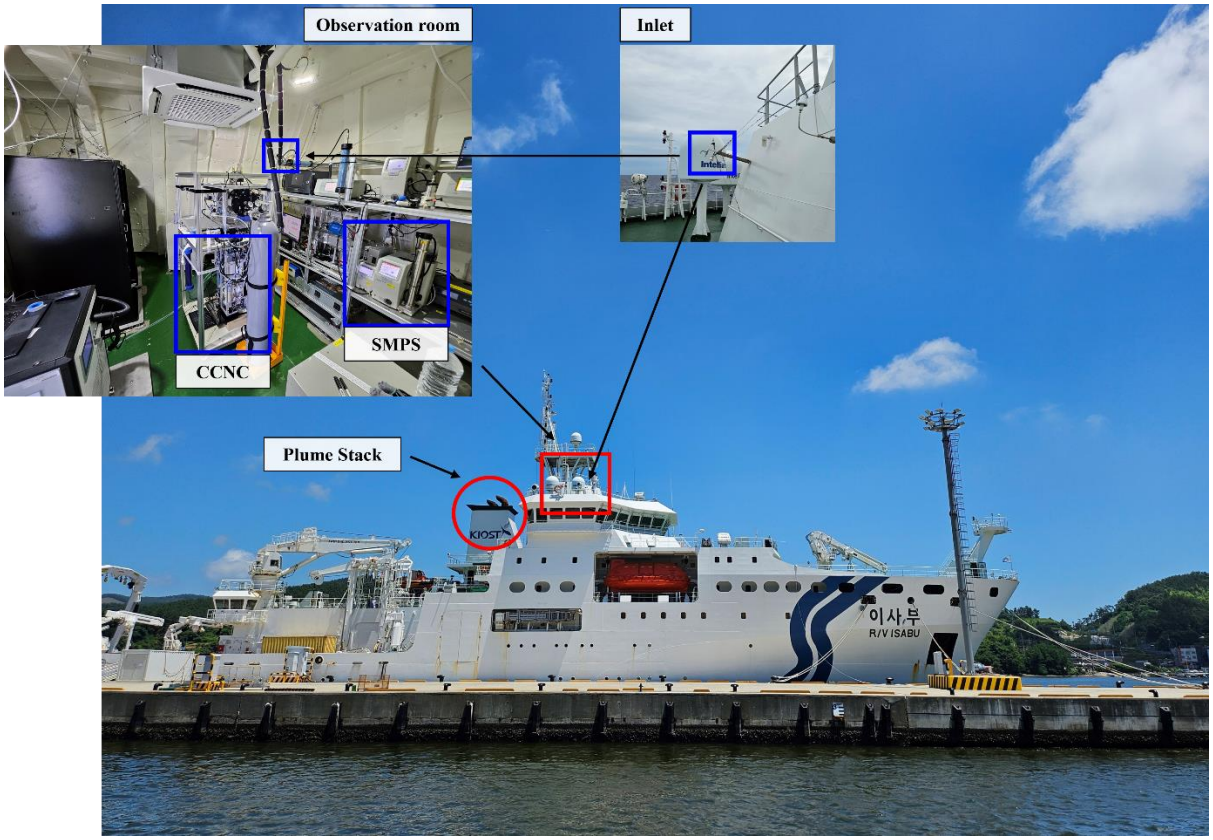

Figure S1. Picture of R/V *ISABU*. The red rectangle denotes the observation room with inlets, and the four blue rectangles in the interior photograph indicate the SMPS, CCNC, and inlets. The red circle represents the vessel's plume stack.

[Comments 19] – Figure 2

Consider labeling the regions along the x-axis, similar to Figure 4, to clearly indicate when the ship is in the East China Sea, South China Sea, Strait of Malacca, and Indian Ocean.

Response:

While the map with regional classification was previously presented in Figure S3, we have merged Figure 2 and Figure S3 following the referee's suggestion. Specifically, the regional classification has been integrated into (new) Figure 1, and Figure S3 has been removed.

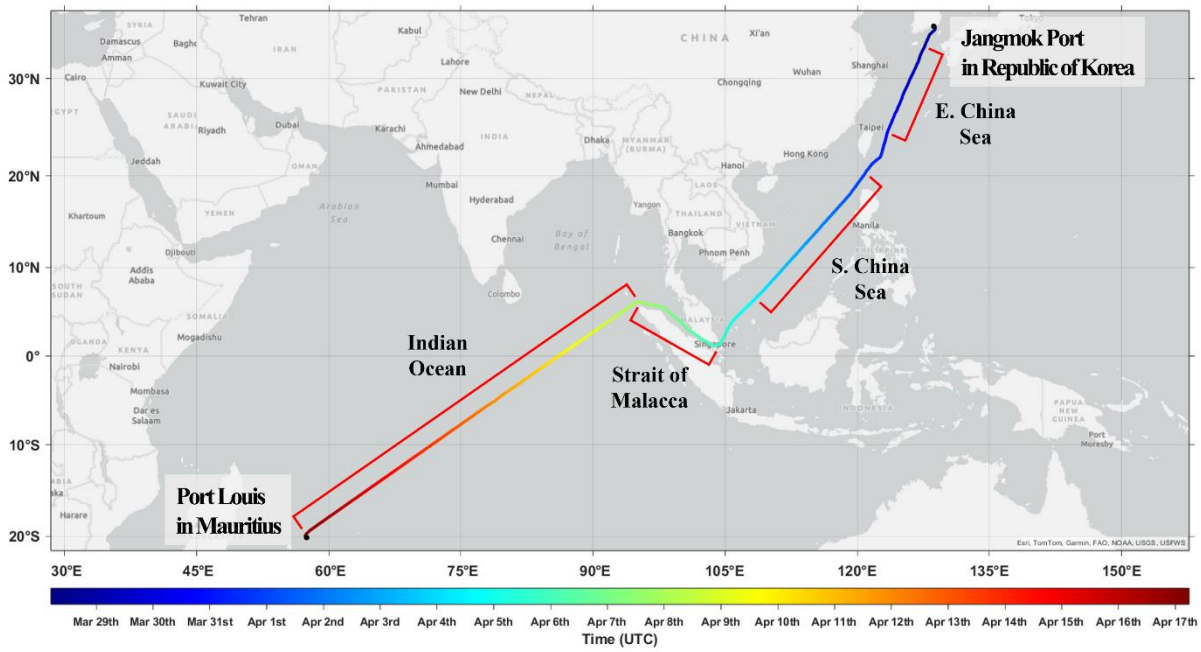

Figure 1. Cruise route of the R/V *ISABU* in 2024, including regional classification (Source: Esri, TomTom, Garmin, FAO, NOAA, USGS, USFWS; Powered by Esri).

[Comments 20] – Figure 5

CN_{15} and Dg should be defined in the main text. Please ensure that all abbreviations are clearly introduced in the text itself, rather than only in the figure captions.

Response:

As the referee pointed out, N_{CN15} and Dg in the figures are not explained in the main text but are only introduced in the captions.

To ensure consistency with the main text, where N_{CN} is used throughout, we revised N_{CN15} to N_{CN} in Figures 3, 4, 5, 7, and 8. Instead, we added a detailed definition of N_{CN} in Section 2.1.2. We also revised the description in these figures' captions to 'total aerosol number concentration.

"Accordingly, N_{CN} in this study refers to the total number concentration of aerosols larger than 15 nm." (lines 152–153)

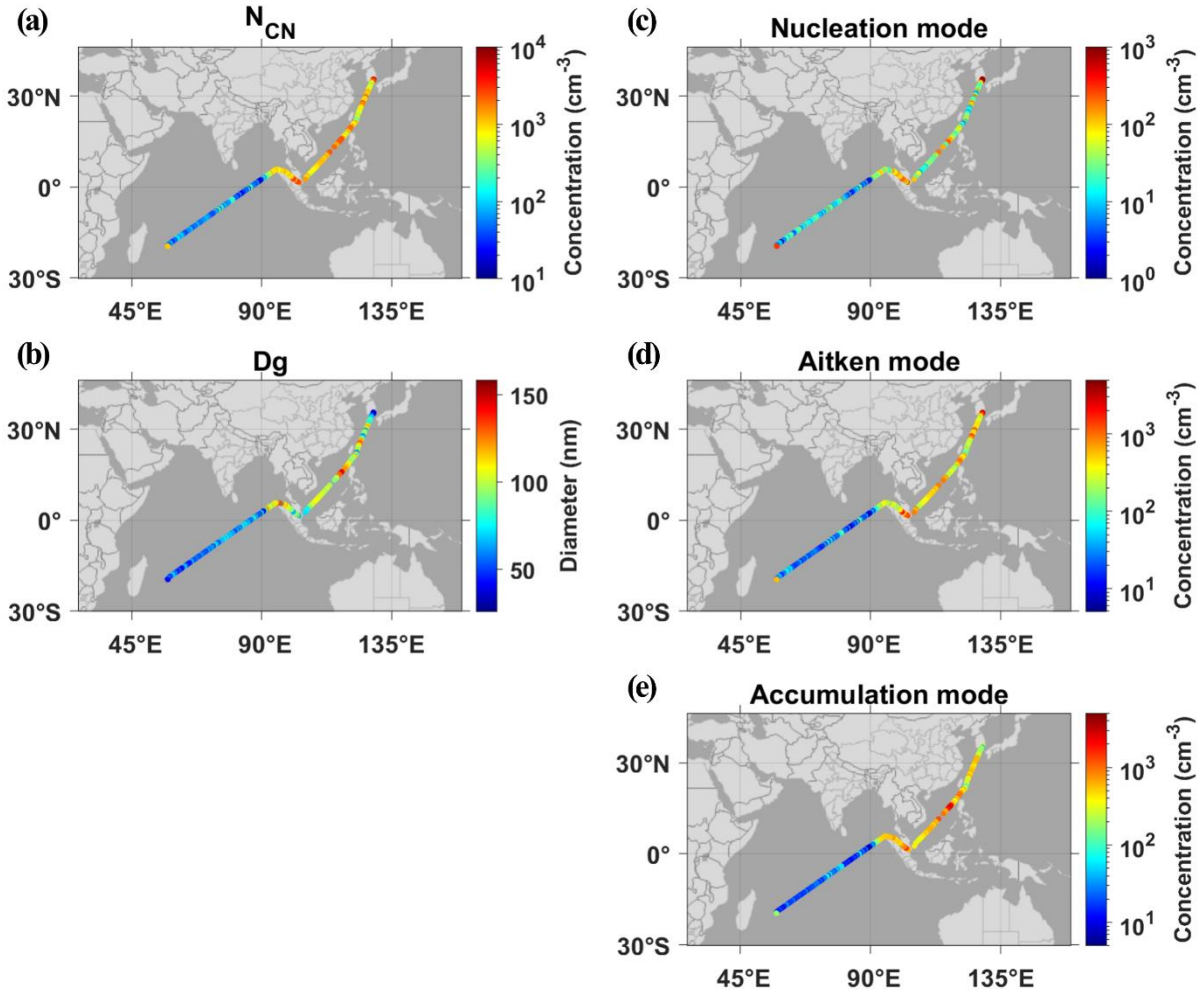

Figure 4. Spatial distributions of (a) total aerosol number concentrations, (b) geometric mean diameter, and number concentrations of (c) nucleation mode (15–25 nm), (d) Aitken mode (25–100 nm), and (e) accumulation mode (100–500 nm) during the transit voyage of the R/V *ISABU* (from Natural Earth).

Meanwhile, for Dg, its definition was added into the sentence where 'geometric mean diameter' first appears. As a result, unlike N_{CN15}, Dg in Figures 4 and 7 remains unchanged.

"In fact, this enhancement was primarily driven by the accumulation mode (Fig. 4e), particularly by particles around 200 nm diameter, consistent with the distribution of geometric mean diameter (Dg) presented in Fig. 4b. A detailed analysis of this phenomenon will be provided in Section 3.1.2." (lines 306–309)

Moreover, in response to the referee's comment, we have thoroughly reviewed all other abbreviations throughout the manuscript and supplement.

[Comments 21] – Figures 8 and 9

Please clarify whether the box plots represent interquartile ranges, and explicitly state this in the figure captions.

Response:

We sincerely appreciate the referee's comments on this critical point. The criteria for the various elements of a box plot must be clearly defined. Accordingly, we have added a description of relevant details used to make box plots to the captions of Fig. 7 and 8. Furthermore, we have updated the captions for the box plots in the supplement to include these details (Fig. S6 and S9).

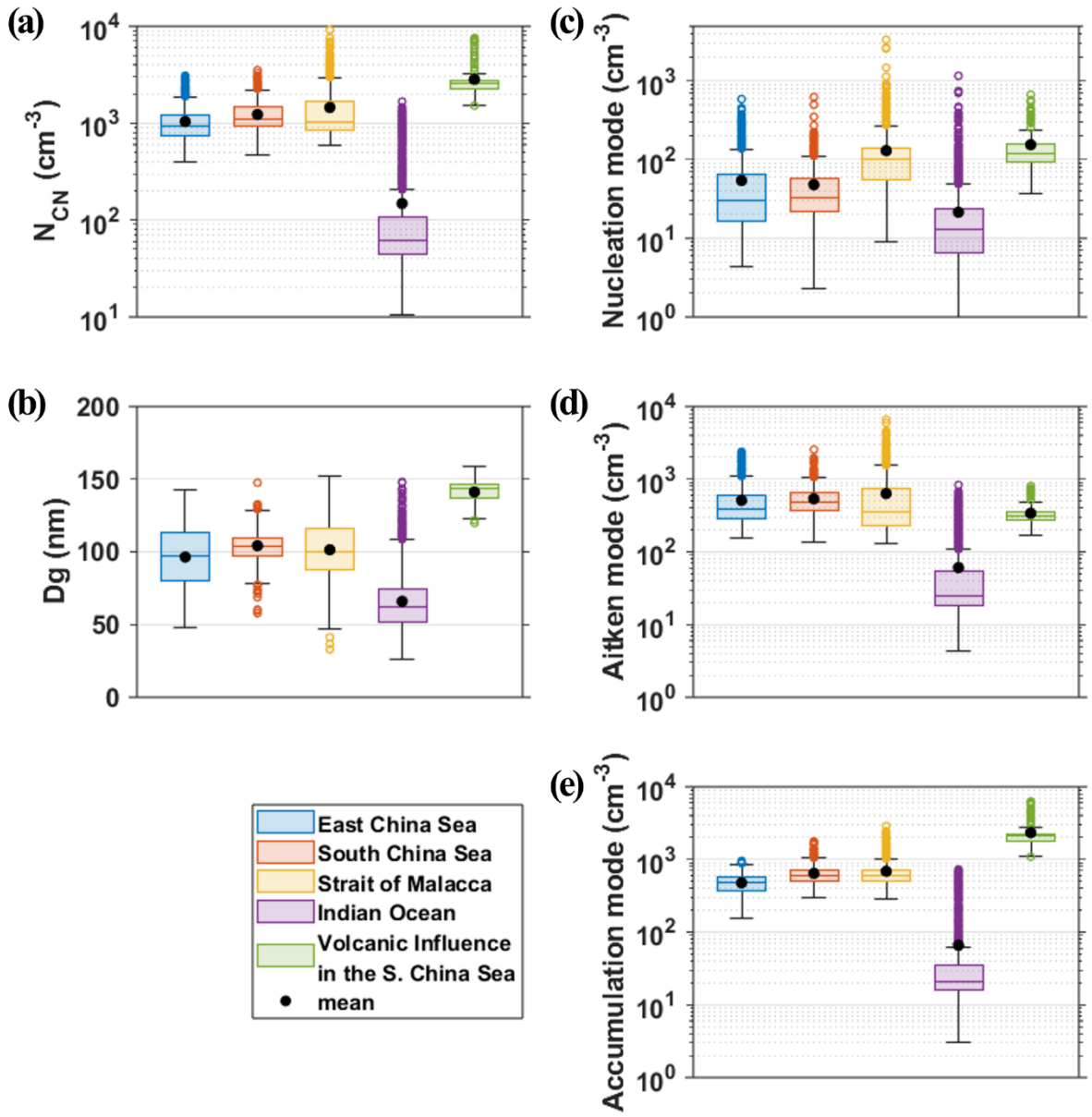

Figure 7. Box plots of (a) total aerosol number concentrations, (b) geometric mean diameter, and (c) nucleation (15–25 nm), (d) Aitken (25–100 nm), and (e) accumulation (100–500 nm) mode number concentrations for each sea area. For the South China Sea, the volcanic-influence period was depicted separately. The horizontal line in each box and the black dots represent the median and mean values, respectively. The range of the boxes is from 25th percentile to 75th percentile (IQR). The whiskers extend away from the box to the two extreme values but if there are data points that exceed $1.5 \times IQR$ from the upper or lower end of the box, they are shown as colored dots as outliers.

[Comments 22] – Figure 9c and 9d

Consider adding more y-axis ticks (e.g., at intervals of 0.2) to improve readability and allow for easier comparison across regions.

Response:

Following the referee's comments, we converted the y-axis ticks for better readability. Consistent with Fig. 8, the y-axis ticks of Fig. S9 have been modified.

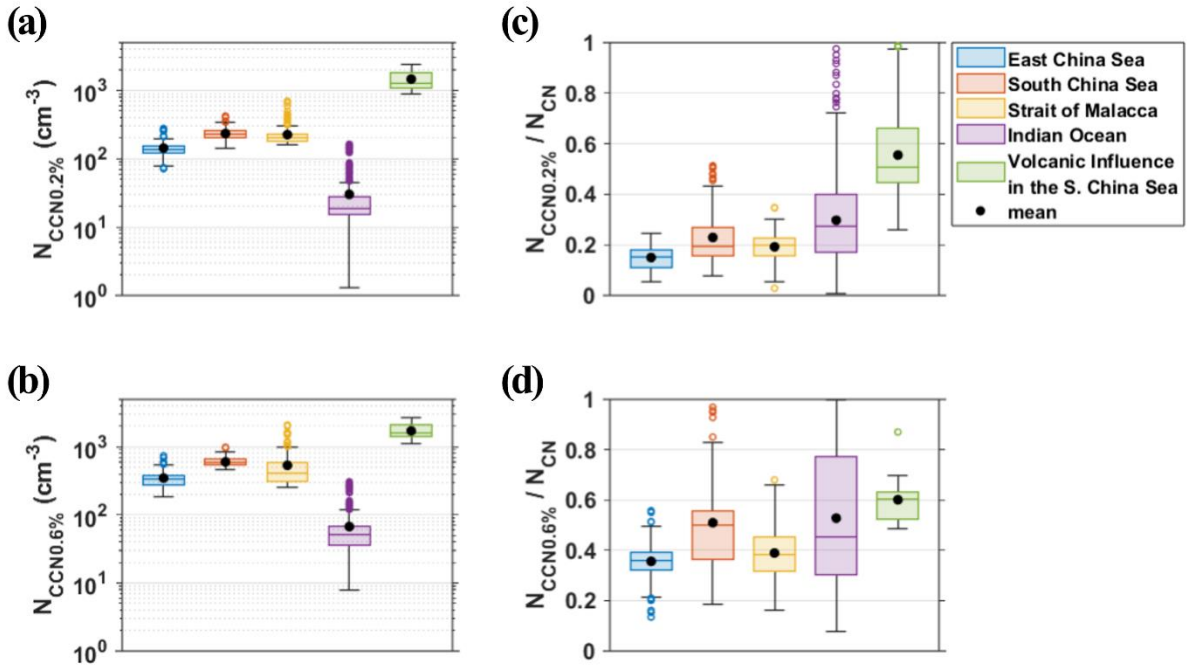

Figure 8. Box plots of (a–b) CCN number concentrations at 0.2% and 0.6% supersaturation and (c–d) their ratios to the total aerosol number concentrations for each sea area. For the South China Sea, the volcanic-influence period was depicted separately. The horizontal line in each box and the black dots represent the median and mean values, respectively. The range of the boxes is from 25th percentile to 75th percentile (IQR). The whiskers extend away from the box to the two extreme values but if there are data points that exceed $1.5 \times IQR$ from the upper or lower end of the box, they are shown as colored dots as outliers.

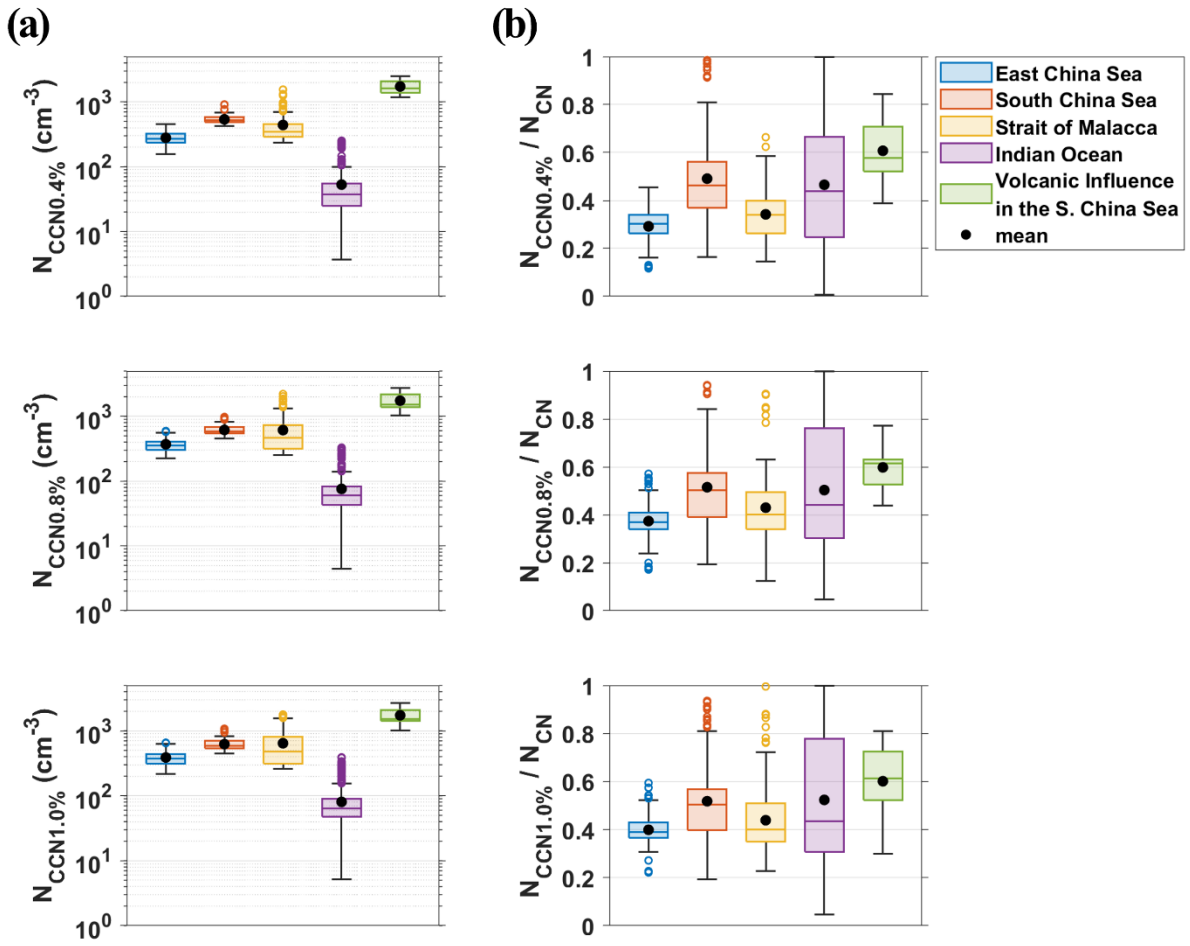

Figure S9. Box plots of (a) CCN number concentrations at 0.4%, 0.8% and 1.0% supersaturation and (b) their ratios to the total aerosol number concentrations for each sea area. For the South China Sea, the volcanic-influence period was depicted separately. The horizontal line in each box and the black dots represent the median and mean values, respectively. The range of the boxes is from 25th percentile to 75th percentile (IQR). The whiskers extend away from the box to the two extreme values but if there are data points that exceed $1.5 \times IQR$ from the upper or lower end of the box, they are shown as colored dots as outliers.

[Comments 23] – SI Line 110

To convert between vacuum diameter and mobility diameter, a typical effective density is between 1–1.6 g/cm^3. Why was 1.7 g/cm^3 assumed?

Response:

First, we apologize for the unclear description.

The density of 1.7 g cm^{-3} was not used for the conversion between vacuum aerodynamic diameter and mobility diameter. Instead, it was used to convert number concentrations into mass concentrations by assuming spherical particles, as described in Equation S6 of the supplement.

Next, the density of 1.7 g cm^{-3} represents the average aerosol density calculated from AMS data during the entire cruise. Admittedly, this value may not be perfectly representative of the total aerosol density since the AMS cannot observe refractory components. However, the key point is to evaluate the consistency between PM2.5 and the mass concentrations derived from SMPS/APS size distribution for validating the SMPS correction. Therefore, we determined that using this value that partially reflects the chemical composition measured during the cruise is more appropriate than using a general literature value. As a result, 1.7 g cm^{-3} was used for the number-to-mass conversion.

To avoid confusion, we revised the relevant sentence in the supplement and added a statement describing the uncertainty with this density assumption.

"To validate the number concentration correction of SMPS, the number concentrations were converted to mass concentrations using Equation S6, assuming spherical particles." (lines 112–113 in supplement)

"where ρ denotes the aerosol density; in this study, we used a value of 1.7 g cm^{-3}, which is the mean aerosol density calculated from the AMS data throughout the entire cruise." (lines 118–119 in supplement)

References

Albrecht, B. A.: Aerosols, Cloud Microphysics and Fractional Cloudiness, Science, 245, 1227–1230, https://doi.org/10.1126/science.245.4923.1227, 1989.

Bellouin, N., Quaas, J., Gryspeerdt, E., Kinne, S., Stier, P., Watson-Parris, D., Boucher, O., Carslaw, K. S., Christensen, M., Daniau, A.-L., Dufresne, J.-L., Feingold, G., Fiedler, S., Forster, P., Gettelman, A., Haywood, J. M., Lohmann, U., Malavelle, F., Mauritsen, T., McCoy, D. T., Myhre, G., Mülmenstädt, J., Neubauer, D., Possner, A., Rugenstein, M., Sato, Y., Schulz, M., Schwartz, S. E., Sourdeval, O., Storelvmo, T., Toll, V., Winker, D., and Stevens, B.: Bounding Global Aerosol Radiative Forcing of Climate Change, Rev. Geophys., 58, e2019RG000660, https://doi.org/10.1029/2019RG000660, 2020.

Carslaw, K. S., Lee, L. A., Reddington, C. L., Pringle, K. J., Rap, A., Forster, P. M., Mann, G. W., Spracklen, D. V., Woodhouse, M. T., Regayre, L. A., and Pierce, J. R.: Large contribution of natural aerosols to uncertainty in indirect forcing, Nature, 503, 67–71, https://doi.org/10.1038/nature12674, 2013.

Chen, Y., Haywood, J., Wang, Y., Malavelle, F., Jordan, G., Peace, A., Partridge, D. G., Cho, N., Oreopoulos, L., Grosvenor, D., Field, P., Allan, R. P., and Lohmann, U.: Substantial cooling effect from aerosol-induced increase in tropical marine cloud cover, Nat. Geosci., 17, 404–410, https://doi.org/10.1038/s41561-024-01427-z, 2024.

Coggon, M. M., Sorooshian, A., Wang, Z., Craven, J. S., Metcalf, A. R., Lin, J. J., Nenes, A., Jonsson, H. H., Flagan, R. C., and Seinfeld, J. H.: Observations of continental biogenic impacts on marine aerosol and clouds off the coast of California, J. Geophys. Res.-Atmos., 119, 6724–6748, https://doi.org/10.1002/2013JD021228, 2014.

Dournaux, M., Tulet, P., Pianezze, J., Brioude, J., Metzger, J.-M., Thyssen, M., and Athier, G.: Origin, size distribution, and hygroscopic properties of marine aerosols in the southwestern Indian Ocean: results of six campaigns of shipborne observations, Atmos. Chem. Phys., 25, 10315–10335, https://doi.org/10.5194/acp-25-10315-2025, 2025.

Dusek, U., Frank, G. P., Hildebrandt, L., Curtius, J., Schneider, J., Walter, S., Chand, D., Drewnick, F., Hings, S., Jung, D., Borrmann, S., Andreae, M. O.: Size Matters More Than Chemistry for Cloud-Nucleating Ability of Aerosol Particles, Science, 312, 1375–1378, https://doi.org/10.1126/science.1125261, 2006.

Fan, J., Wang, Y., Rosenfeld, D., and Liu, X.: Review of Aerosol–Cloud Interactions: Mechanisms, Significance, and Challenges, J. Atmos. Sci., 73, 4221–4252, https://doi.org/10.1175/JAS-D-16-0037.1, 2016.

Forster, P., Storelvmo, T., Armour, K., Collins, W., Dufresne, J.-L., Frame, D., Lunt, D. J., Mauritsen, T., Palmer, M. D., Watanabe, M., Wild, M., and Zhang, H.: The Earth's Energy Budget, Climate Feedbacks, and Climate Sensitivity, in: Climate Change 2021: The Physical Science Basis, Contribution of Working Group I to the Sixth Assessment Report of the Intergovernmental Panel on Climate Change, edited by: Masson-Delmotte, V., Zhai, P., Pirani, A., et al., Cambridge University Press, Cambridge, UK and New York, NY, USA, 923–1054,

https://doi.org/10.1017/9781009157896.009, 2021.

Gaston, C. J., Cahill, J. F., Collins, D. B., Suski, K. J., Ge, J. Y., Barkley, A. E., and Prather, K. A.: The Cloud Nucleating Properties and Mixing State of Marine Aerosols Sampled along the Southern California Coast, Atmosphere, 9, 52, https://doi.org/10.3390/atmos9020052, 2018.

Gong, J., Zhu, Y., Chen, D., Gao, H., Shen, Y., Gao, Y., and Yao, X.: The occurrence of lower-than-expected bulk N_{CCN} values over the marginal seas of China – Implications for competitive activation of marine aerosols, Sci. Total Environ., 858, 159938, https://doi.org/10.1016/j.scitotenv.2022.159938, 2023.

King, S. M., Butcher, A. C., Rosenoern, T., Coz, E., Lieke, K. I., de Leeuw, G., Nilsson, E. D., and Bilde, M.: Investigating Primary Marine Aerosol Properties: CCN Activity of Sea Salt and Mixed Inorganic-Organic Particles, Environ. Sci. Technol., 46, 10405–10412, https://doi.org/10.1021/es300574u, 2012.

Martin, M., Chang, R. Y.-W., Sierau, B., Sjogren, S., Swietlicki, E., Abbatt, J. P. D., Leck, C., and Lohmann, U.: Cloud condensation nuclei closure study on summer arctic aerosol, Atmos. Chem. Phys., 11, 11335–11350, https://doi.org/10.5194/acp-11-11335-2011, 2011.

Modini, R. L., Frossard, A. A., Ahlm, L., Russell, L. M., Corrigan, C. E., Roberts, G. C., Hawkins, L. N., Schroder, J. C., Bertram, A. K., Zhao, R., Lee, A. K. Y., Abbatt, J. P. D., Lin, J., Nenes, A., Wang, Z., Wonaschütz, A., Sorooshian, A., Noone, K. J., Jonsson, H., Seinfeld, J. H., Toom-Sauntry, D., Macdonald, A. M., and Leaitch, W. R.: Primary marine aerosol-cloud interactions off the coast of California, J. Geophys. Res.-Atmos., 120, 42824303, https://doi.org/10.1002/2014JD022963, 2015.

Nair, V. S., Ajith, T. C., Jayachandran, V. N., Kompalli, S. K., Gogoi, M. M., and Babu, S. S.: Effects of South Asian outflow on aerosol hygroscopicity and cloud droplet activation over the northern Indian Ocean, Atmos. Environ., 327, 120500, https://doi.org/10.1016/j.atmosenv.2024.120500, 2024.

Ou, H., Cai, M., Zhang, Y., Ni, X., Liang, B., Sun, Q., Mai, S., Sun, C., Zhou, S., Wang, H., Sun, J., and Zhao, J.: Measurement report: Cloud condensation nuclei (CCN) activity in the South China Sea from shipborne observations during the summer and winter of 2021 – seasonal variation and anthropogenic influence, Atmos. Chem. Phys., 25, 2495–2513, https://doi.org/10.5194/acp-25-2495-2025, 2025.

Park, J., Dall'Osto, M., Park, K., Gim, Y., Kang, H. J., Jang, E., Park, K.-T., Park, M., Yum, S. S., Jung, J., Lee, B. Y., and Yoon, Y. J.: Shipborne observations reveal contrasting Arctic marine, Arctic terrestrial and Pacific marine aerosol properties, Atmos. Chem. Phys., 20, 5573–5590, https://doi.org/10.5194/acp-20-5573-2020, 2020.

Park, K.-T., Yoon, Y. J., Lee, K., Tunved, P., Krejci, R., Ström, J., Jang, E., Kang, H. J., Jang, S., Park, J., Lee, B. Y., Traversi, R., Becagli, S., and Hermansen, O.: Dimethyl Sulfide-Induced Increase in Cloud Condensation Nuclei in the Arctic Atmosphere, Global Biogeochem. Cy., 35, e2021GB006969, https://doi.org/10.1029/2021GB006969, 2021.

Petters, M. D. and Kreidenweis, S. M.: A single parameter representation of hygroscopic growth and cloud condensation nucleus activity, Atmos. Chem. Phys., 7, 1961–1971, https://doi.org/10.5194/acp-7-1961-2007, 2007.

Sanchez, K. J., Chen, C.-L., Russell, L. M., Betha, R., Liu, J., Price, D. J., Massoli, P., Ziemba, L. D., Crosbie, E. C., Moore, R. H., Müller, M., Schiller, S. A., Wisthaler, A., Lee, A. K. Y., Quinn, P. K., Bates, T. S., Porter, J., Bell, T. G., Saltzman, E. S., Vaillancourt, R. D., and Behrenfeld, M. J.: Substantial Seasonal Contribution of Observed Biogenic Sulfate Particles to Cloud Condensation Nuclei, Sci. Rep., 8, 3235, https://doi.org/10.1038/s41598-018-21590-9, 2018.

Sanchez, K. J., Roberts, G. C., Saliba, G., Russell, L. M., Twohy, C., Reeves, J. M., Humphries, R. S., Keywood, M. D., Ward, J. P., and McRobert, I. M.: Measurement report: Cloud processes and the transport of biological emissions affect southern ocean particle and cloud condensation nuclei concentrations, Atmos. Chem. Phys., 21, 3427–3446, https://doi.org/10.5194/acp-21-3427-2021, 2021.

Tatzelt, C., Henning, S., Welti, A., Baccarini, A., Hartmann, M., Gysel-Beer, M., van Pinxteren, M., Modihi, R. L., Schmale, J., and Stratmann, F.: Circum-Antarctic abundance and properties of CCN and INPs, Atmos. Chem. Phys., 22, 9721–9745, https://doi.org/10.5194/acp-22-9721-2022, 2022.

Twomey, S.: Pollution and the planetary albedo, Atmos. Environ., 8, 1251–1256, https://doi.org/10.1016/0004-6981(74)90004-3, 1974.

Uin, J. and Enekwizu, O. Y. Cloud condensation Nuclei Particle Counter Instrument Handbook, U.S. Department of Energy, Atmospheric Radiation Measurement user facility, Richland, Washington, DOE/SC-ARM-TR-168, https://doi.org/10.2172/1251411, 2024.

Wiedensohler, A., Wiesner, A., Weinhold, K., Birmili, W., Hermann, M., Merkel, M., Müller, T., Pfeifer, S., Schmidt, A., Tuch, T., Velarde, F., Quincey, P., Seeger, S., and Nowak, A.: Mobility Particle Size Spectrometers: Calibration Procedures and Measurement Uncertainties, Aerosol Sci. Technol., 52, 146–164, https://doi.org/10.1080/02786826.2017.1387229, 2017.

Wood, R., Wyant, M., Bretherton, C. S., Rémillard, J., Kollias, P., Fletcher, J., Stemmler, J., de Szoeke, S., Yuter, S., Miller, M., Mechem, D., Tselioudis, G., Chiu, J. C., Mann, J. A. L., O'Connor, E. J., Hogan, R. J., Dong, X., Miller, M., Ghate, V., Jefferson, A., Min, Q., Minnis, P., Palikonda, R., Albrecht, B., Luke, E., Hannay, C., and Lin, Y.: Clouds, Aerosols, and Precipitation in the Marine Boundary Layer: An ARM Mobile Facility Deployment, B. Am. Meteorol. Soc., 96, 419–440, https://doi.org/10.1175/BAMS-D-13-00180.1, 2015.